Rational design, synthesis and evaluation of uncharged, "smart" *bis*-oxime antidotes of OP inhibited human acetylcholinesterase

Lukas Gorecki,[1,a] Oksana Gerlits,[2,b] Xiaotian Kong,[3] Xiaolin Cheng,[3] Donald Blumenthal,[4] Palmer Taylor,[1] Carlo Ballatore,[1] Andrey Kovalevsky,[5] Zoran Radić[1*]

[1]Skaggs School of Pharmacy and Pharmaceutical Sciences, University of California San Diego, La Jolla, CA 92093-0751.
[2]Bredesen Center, University of Tennessee, Knoxville, Tennessee 37996, United States
[3]Division of Medicinal Chemistry & Pharmacognosy, College of Pharmacy, The Ohio State University, Columbus, OH 43210
[4]Department of Pharmacology and Toxicology, University of Utah, Salt Lake City, UT 84112
[5]Neutron Scattering Division, Oak Ridge National Laboratory, Oak Ridge, TN 37831

Running title: *Uncharged* bis-*oxime antidotes of OP inhibited hAChE*

[a]Permanent address: Department of Toxicology and Military Pharmacy, Faculty of Military Health Sciences University of Defence, Trebesska 1575, 500 01 Hradec Kralove, Czech Republic
[b]Present address: Tennessee Wesleyan University, Athens, TN 37303, United States

*Corresponding author, zradic@ucsd.edu. Tel. (858)534-8241

Supporting information

1. General synthetic methods

All solvents were reagent grade. All reagents were purchased from Aldrich or Fisher Scientific and used as received. Thin layer chromatography (TLC) was performed with 0.25 mm E. Merck pre-coated silica gel plates. Flash chromatography was performed with silica gel 60 (particle size 0.040–0.062 mm) supplied by Silicycle and Sorbent Technologies. TLC spots were detected by viewing under a UV light, or using $KMnO_4$ or ceric ammonium molybdate stains. Proton (^1H) and carbon (^{13}C) NMR spectra were recorded on a Varian (600 MHz for ^1H and 151 MHz for ^{13}C). Chemical shifts were reported in δ ppm relative to the residual solvent's peak. ^{13}C carbon NMR was measured as C_deptq. Biotage® Initiator+ was used for microwave irradiation. The final compounds were analyzed by LC-MS and HRMS, Agilent 6230 Accurate-Mass TOFMS system features Agilent Jet Stream Thermal

Focusing technology for significantly improved sensitivity, as well as enhanced MassHunter Workstation software for superior data mining and analysis capabilities and Micromass Quattro Ultima, high performance benchtop triple quadrupole mass spectrometer designed for routine LC-MS and LC-MS/MS operations to obtain high resolution mass spectra. Gradient LC analysis confirmed > 95% purity.

2. Synthesis of novel compounds

2.1. Preparation of oxime fragment

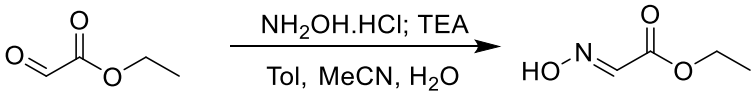

1 **2**

Ethyl (2*E*)-2-(hydroxyimino)acetate (2): Prepared as previously described (1), hydroxylamine hydrochloride ($NH_2OH.HCl$) (1.0 eq; 50.44 mmol) was dissolved in acetonitrile/water (9:1 ratio = 36:4 mL) and ethyl glyoxalate **1** (50% solution in toluene) (1.0 eq; 50.44 mmol) was slowly added. After 10 min of stirring triethylamine (TEA) (1.0 eq; 50.44 mmol) was drop wise introduced over 30 min. The reaction mixture was stirred at room temperature (RT) for 24 hours. Then it was concentrated and diluted with H_2O. The aqueous solution was three times washed by dichloromethane (DCM) 3x 100 mL and the organic phases were collected, dried over anhydrous sodium sulfate (Na_2SO_4), filtered and concentrated to give crude product as colorless oil. Yield 61%.

^{1}H NMR (600 MHz, DMSO-d_6) δ 12.56 (s, 1H), 7.54 (s, 1H), 4.19 (q, J = 7.1 Hz, 2H), 1.23 (t, J = 7.1 Hz, 3H). ^{13}C NMR (151 MHz, DMSO-d_6) δ 162.45, 141.12, 60.85, 14.19.

2.2. General procedure A: *N*-alkylation with 2-chloroacetonitrile

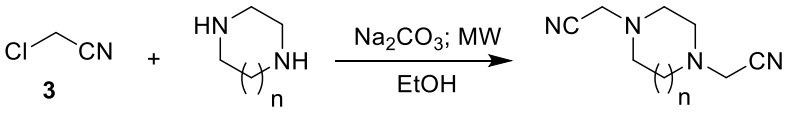

4 n = 1
5 n = 2

6 n = 1
7 n = 2

Piperazine **4** or homopiperazine **5** (1.0 eq); 2-chloroacetonitrile **3** (2.4 eq) and Na_2CO_3 (4.0 eq) were dissolved in absolute EtOH. The reaction mixture was challenged by microwave (MW) irradiation for 5 hours at 100 °C (dynamic curve with power up to 200 W). The solid

was filtered and the filtrate was purified by column chromatography using mobile phase DCM and methanol (MeOH).

2-[4-(cyanomethyl)piperazin-1-yl]acetonitrile (6): Prepared according to the general procedure A. Piperazine **4** (538 mg; 6.246 mmol); 2-chloroacetonitrile **3** (950 µL; 14.99 mmol); Na_2CO_3 (2.648 g; 24.98 mmol) and EtOH (4 mL). Purification was carried out using mobile phase DCM/MeOH (98:2) to give crude product **6** as yellow oil. Yield 59%.

^{1}H NMR (600 MHz, $CDCl_3$) δ 3.55 (s, 4H), 2.67 (s, 8H). ^{13}C NMR (151 MHz, $CDCl_3$) δ 114.62, 51.36, 46.03.

2-[4-(cyanomethyl)-1,4-diazepan-1-yl]acetonitrile (7): Prepared according to the general procedure A. Homopiperazine **5** (638 mg; 6.37 mmol); 2-chloroacetonitrile **3** (970 µL; 15.29 mmol); Na_2CO_3 (2.701 g; 25.48 mmol) and EtOH (4 mL). Purification was carried out using mobile phase DCM/MeOH (98:2) to give crude product **7** as yellow oil. Yield 81%.

^{1}H NMR (600 MHz, $CDCl_3$) δ 3.58 (s, 4H), 2.88 – 2.74 (m, 8H), 1.96 – 1.86 (m, 2H). ^{13}C NMR (151 MHz, $CDCl_3$) δ 115.78, 54.39, 53.47, 47.34, 27.86.

2.3. The *N*-alkylation with 3-bromopropionitrile

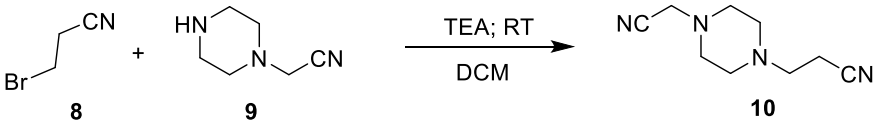

3-[4-(cyanomethyl)piperazin-1-yl]propanenitrile (10): The intermediate **9** (974 mg; 7.78 mmol) was dissolved in anhydrous DCM (15 mL) and 3-bromopropionitrile **8** (645 µL; 7.78 mmol) was added. After 10 min of stirring, TEA (2.17 mL; 15.56 mmol) was drop wise introduced. The reaction mixture was stirred at RT for 24 hours. The solution was diluted with H_2O, the organic phase was removed and water phase was extracted with DCM (3x 50 mL). The combined organic layers were dried over Na_2SO_4, filtered, concentrated and purified by column chromatography using mobile phase DCM/MeOH (14:1) to give **10** as dark yellow oil. Yield 66%.

^{1}H NMR (600 MHz, $CDCl_3$) δ 3.52 (s, 2H), 2.72 (t, *J* = 7.0 Hz, 2H), 2.69 – 2.55 (m, 8H), 2.52 (t, *J* = 7.0 Hz, 2H). ^{13}C NMR (151 MHz, $CDCl_3$) δ 118.62, 114.62, 53.08, 52.12, 51.56, 45.82, 15.99.

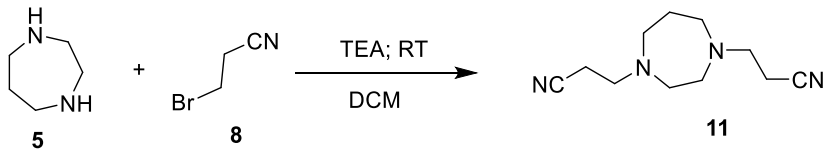

3-[4-(2-cyanoethyl)-1,4-diazepan-1-yl]propanenitrile (11): Homopiperazine **5** (1.803 mg; 18.0 mmol) was dissolved in anhydrous DCM (20 mL) and 3-bromopropionitrile **8** (2.986 mL; 36.0 mmol) was added. After 10 min of stirring, TEA (10.0 mL; 72.0 mmol) was added dropwise. The reaction mixture was stirred at RT for 24 hours. The solution was diluted with H_2O, the organic phase was removed and water phase was extracted with DCM (3x 50 mL). The combined organic layers were dried over Na_2SO_4, filtered, concentrated and purified by column chromatography using mobile phase DCM/MeOH (9:1) to give **11** as dark yellow oil. Yield 84%.

^{1}H NMR (600 MHz, $CDCl_3$) δ 2.87 (t, *J* = 6.9 Hz, 4H), 2.80 – 2.71 (m, 8H), 2.47 (t, *J* = 6.9 Hz, 4H), 1.80 (p, *J* = 6.9, 5.3 Hz, 2H). ^{13}C NMR (151 MHz, $CDCl_3$) δ 119.01, 54.74, 53.38, 53.31, 27.98, 16.47.

2.4. Multistep reactions for asymmetric compounds

2.4.1. Preparation of intermediate 9

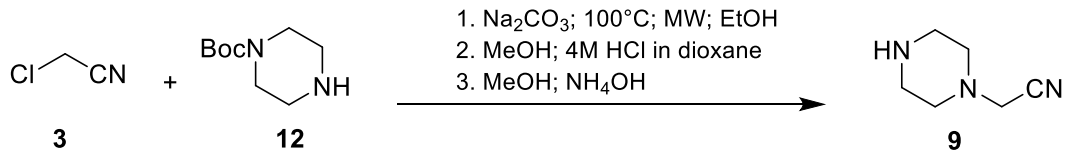

2-(piperazin-1-yl)acetonitrile (9): To a stirred solution of *N*-Boc-piperazine **12** (2.012 g; 10.8 mmol) in absolute EtOH (10 mL), 2-chloroacetonitrile **3** (820 µL; 13.0 mmol) and Na_2CO_3 (2.289 g; 21.6 mmol) were subsequently added. The reaction mixture was challenged by MW irradiation for 5 hours at 100 °C (dynamic curve with power up to 200 W). The solution was concentrated, diluted with H_2O and extracted with DCM (3x 50 mL). The combined organic layers were dried over Na_2SO_4, filtered, concentrated and used into next step without any further purification.

The residue was dissolved in MeOH (30 mL) and 1 M solution of HCl in dioxane (15 mL) was slowly added. The mixture was stirred at RT for 20 hours. The result was concentrated

and dried under reduced pressure. The residue was re-dissolved in MeOH (30 mL) and 25% solution of ammonium hydroxide (NH_4OH) in water (15 mL) was added. After another 1 hour of stirring the reaction mixture was concentrated and directly purified by column chromatography using mobile phase DCM/MeOH/NH_4OH (6:1:0.1) to give **9** as yellow oil. Yield 72% after two steps.

^{1}H NMR (600 MHz, $CDCl_3$) δ 3.50 (s, 2H), 2.93 (t, *J* = 4.9 Hz, 4H), 2.55 (t, *J* = 4.9 Hz, 4H), 1.74 (bs, 1H). ^{13}C NMR (151 MHz, $CDCl_3$) δ 114.66, 52.93, 46.56, 45.54.

2.4.2. Preparation of *N,N'*-piperidine *bis*-alkylcarbonitriles:

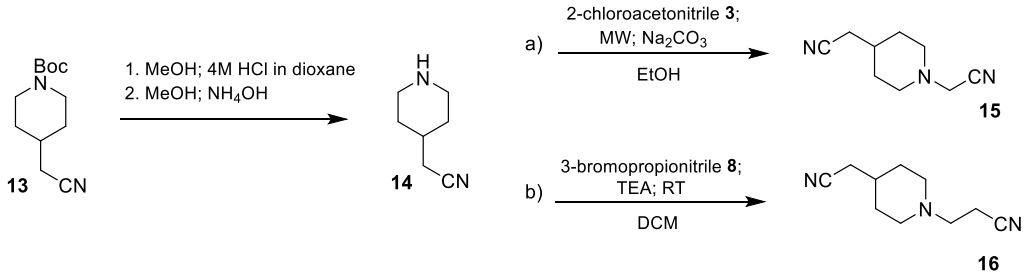

To a solution of *N*-Boc-4-cyanomethylpiperidine **13** (4.118 g; 18.36 mmol) in MeOH (20 mL), a 1 M solution of HCl in dioxane (10 mL) was slowly added. The mixture was stirred at RT for 20 hours. The result was concentrated and dried under reduced pressure. The residue was re-dissolved in MeOH (20 mL) and 25% solution of ammonium hydroxide (NH_4OH) in water (10 mL) was added. After another 1 hour of stirring the reaction mixture was concentrated and directly purified using column chromatography with mobile phase DCM/MeOH/NH_4OH (6:1:0.1) to give 4-cyanomethylpiperidine **14** as white solid in quantitative yield. The amount of **9** was halved and used into next steps without any characterization.

a) **2-[1-(cyanomethyl)piperidin-4-yl]acetonitrile (15):** To a solution of 4-cyanomethylpiperidine **14** (1.14 g; 9.18 mmol) in absolute EtOH (10 mL), 2-chloroacetonitrile **3** (700 µL; 11.0 mmol) and Na_2CO_3 (1.946 g; 18.36 mmol) were subsequently added. The reaction mixture was challenged by MW irradiation for 10 hours at 100 °C (dynamic curve with power up to 200 W). The result was concentrated and directly purified using column chromatography with mobile phase DCM/MeOH (95:5) to give **15** as yellowish solid. Yield 62% after 2 steps.

^{1}H NMR (600 MHz, $CDCl_3$) δ 3.68 (s, 2H), 3.03 – 2.94 (m, 2H), 2.54 – 2.49 (m, 2H), 2.47 (d, *J* = 6.8 Hz, 2H), 2.06 – 1.97 (m, 2H), 1.91 – 1.81 (m, 1H), 1.65 – 1.54 (m, 2H). ^{13}C NMR (151 MHz, $CDCl_3$) δ 118.16, 114.60, 51.64, 46.22, 32.04, 31.09, 23.83.

b) **3-[4-(cyanomethyl)piperidin-1-yl]propanenitrile (16):** To a solution of 4-cyanomethylpiperidine **14** (1.14 g; 9.18 mmol) in anhydrous DCM (25 mL), 3-bromopropionitrile **8** (913 µL; 11.0 mmol) was added. After 10 min of stirring, TEA (2.6 mL; 18.36 mmol) was added dropwise. The reaction mixture was stirred at RT for 24 hours. The solution was diluted with H_2O, the organic phase was removed and water phase was extracted with DCM (3x 30 mL). The combined organic phases were dried over Na_2SO_4, filtered, concentrated and purified by column chromatography using mobile phase DCM/MeOH (95:5) to give **16** as yellow oil. Yield 79% after two steps.

^{1}H NMR (600 MHz, $CDCl_3$) δ 3.08 – 2.99 (m, 2H), 2.80 (t, *J* = 7.1 Hz, 2H), 2.62 (t, *J* = 7.0 Hz, 2H), 2.42 (d, *J* = 7.0 Hz, 2H), 2.27 – 2.16 (m, 2H), 1.99 – 1.89 (m, 2H), 1.86 – 1.73 (m, 1H), 1.61 – 1.45 (m, 2H). ^{13}C NMR (151 MHz, $CDCl_3$) δ 118.89, 118.44, 53.34, 52.59, 32.87, 31.37, 23.88, 15.96.

2.5. General procedure B: reduction of carbonitriles using $LiAlH_4$

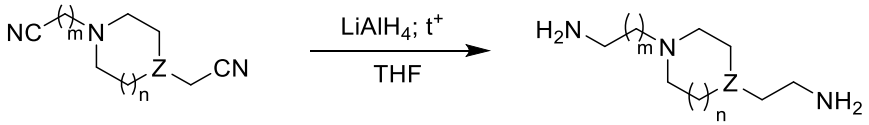

6 Z = N; n = 1; m = 1
7 Z = N; n = 2; m = 1
10 Z = N; n = 1; m = 2
15 Z = C; n = 1; m = 1

17 Z = N; n = 1; m = 1
18 Z = N; n = 2; m = 1
19 Z = N; n = 1; m = 2
20 Z = C; n = 1; m = 1

A 4 M solution of $LiAlH_4$ in Et_2O (4.6 eq) was added into anhydrous THF (20 mL) under N_2 atmosphere. The appropriate *bis*-nitrile (1.0 eq) dissolved in anhydrous THF (20 mL) was then added dropwise to the solution of $LiAlH_4$. The reaction mixture was heated to 90 °C for 4 hours. The reaction mixture was cooled to 0 °C and slowly neutralized by addition of H_2O and then by addition of 10% solution of NaOH. The solid was filtered and the filtrate was directly purified by column chromatography using mobile phase DCM/MeOH/NH_4OH (6:3:1) to give the desired product (**17-20**).

2-[4-(2-aminoethyl)piperazin-1-yl]ethan-1-amine (17): Prepared as previously described (2) according to the general procedure B. Compound **6** (585 mg; 3.56 mmol); $LiAlH_4$ (4 M in

Et_2O) (4.1 mL; 16.4 mmol) and neutralization by 1 mL H_2O and 3 mL of 10% NaOH. Quantitative yield, product **17** as dark yellow oil.

^{1}H NMR (600 MHz, $CDCl_3$) δ 2.78 (t, *J* = 6.2 Hz, 8H), 2.48 (bs, 4H), 2.41 (t, *J* = 6.2 Hz, 8H). ^{13}C NMR (151 MHz, $CDCl_3$) δ 61.34, 53.49, 38.97.

3-[4-(2-aminoethyl)piperazin-1-yl]propan-1-amine (19): Prepared according to the general procedure B. Compound **10** (921 mg; 5.17 mmol); $LiAlH_4$ (4 M in Et_2O) (6.5 mL; 25.85 mmol) and neutralization by 2 mL H_2O and 4.5 mL of 10% NaOH. Yield 61%, product **19** as dark yellow oil.

^{1}H NMR (600 MHz, $CDCl_3$) δ 2.88 (t, *J* = 4.9 Hz, 2H), 2.81 – 2.71 (m, 4H), 2.52 – 2.34 (m, 10H), 1.66 – 1.61 (m, 2H). ^{13}C NMR (151 MHz, $CDCl_3$) δ 61.77, 61.15, 56.52, 46.10, 40.84, 38.79, 30.43.

2-[4-(2-aminoethyl)-1,4-diazepan-1-yl]ethan-1-amine (18): Prepared according to the general procedure B. The compound **7** (785 mg; 4.4 mmol); $LiAlH_4$ (4 M in Et_2O) (5.0 mL; 20.26 mmol) and neutralization by 1 mL H_2O and 4 mL of 10% NaOH. Yield 84%, product **18** as dark yellow oil.

^{1}H NMR (600 MHz, $CDCl_3$) δ 2.75 – 2.71 (m, 4H), 2.70 – 2.64 (m, 8H), 2.55 – 2.51 (m, 4H), 1.80 – 1.74 (m, 2H). ^{13}C NMR (151 MHz, $CDCl_3$) δ 60.83, 55.42, 54.38, 39.58, 27.81.

2-[1-(2-aminoethyl)piperidin-4-yl]ethan-1-amine (20): Prepared according to the general procedure B. The compound **15** (684 mg; 4.19 mmol); $LiAlH_4$ (4 M in Et_2O) (4.8 mL; 19.3 mmol) and neutralization by 1 mL H_2O and 4 mL of 10% NaOH. Yield 82%, product **20** as dark yellow oil.

^{1}H NMR (600 MHz, DMSO-d_6) δ 2.91 (dt, *J* = 11.7, 3.4 Hz, 2H), 2.71 (t, *J* = 6.6 Hz, 2H), 2.69 – 2.63 (m, 2H), 2.38 (t, *J* = 6.6 Hz, 2H), 1.97 (td, *J* = 11.7, 2.5 Hz, 2H), 1.75 – 1.67 (m, 2H), 1.45 – 1.35 (m, 3H), 1.28 – 1.17 (m, 2H). ^{13}C NMR (151 MHz, DMSO-d_6) δ 61.72, 54.13, 40.04, 39.90, 39.76, 39.62, 39.48, 39.30, 39.09, 32.50.

2.6. General procedure C: reduction of carbonitriles using Raney-nickel

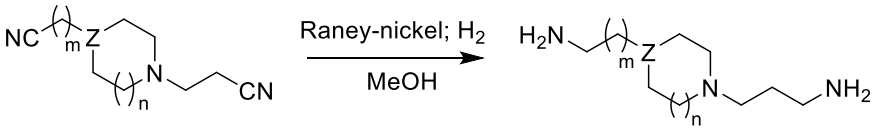

11 Z = N; n = 2; m = 2
16 Z = C; n = 1; m = 1

21 Z = N; n = 2; m = 2
22 Z = C; n = 1; m = 1

To a solution of **11** or **16** (1.0 eq) in anhydrous MeOH under N_2 atmosphere, Raney-nickel (10.0 eq) was added. The resulting mixture was flushed repeatedly with N_2 and then again with H_2. The reaction mixture was stirred under H_2 atmosphere and monitored by TLC. Upon complete consumption of starting material, the reaction mixture was carefully filtered and the filtrate was directly purified by column chromatography using mobile phase DCM/MeOH/NH_4OH (6:3:1) to give the desired product (**21** or **22**).

3-[4-(3-aminopropyl)-1,4-diazepan-1-yl]propan-1-amine (21): Prepared according to the general procedure C. Compound **11** (1.417 g; 6.87 mmol) and Raney-nickel (2800, slurry, in H_2O) (4.03 g; 68.7 mmol) in MeOH 50 mL was stirred for 24 hours. Yield 92%, product **21** as dark yellow oil.

^{1}H NMR (600 MHz, $CDCl_3$) δ 2.85 (t, *J* = 6.8 Hz, 4H), 2.82 – 2.77 (m, 8H), 2.67 – 2.59 (m, 4H), 1.95 – 1.86 (m, 2H), 1.74 (p, *J* = 7.0 Hz, 4H). ^{13}C NMR (151 MHz, $CDCl_3$) δ 56.19, 54.97, 54.35, 40.62, 30.98, 27.19. HRMS (ESI^+): $[M+H]^+$: calculated for $C_{11}H_{27}N_4^+$ (m/z): 215.2230; detected: 215.2234.

3-[4-(2-aminoethyl)piperidin-1-yl]propan-1-amine (22): Prepared according to the general procedure C. Compound **16** (1.094 g; 6.17 mmol) and Raney-nickel (2800, slurry, in H_2O) (3.621 g; 61.7 mmol) in MeOH 30 mL was stirred for 4 hours. Yield 73%, product **22** as dark yellow oil.

^{1}H NMR (600 MHz, $CDCl_3$) δ 3.10 – 2.97 (m, 2H), 2.90 – 2.68 (m, 4H), 2.53 – 2.42 (m, 2H), 2.04 – 1.95 (m, 2H), 1.84 – 1.58 (m, 8H), 1.57 – 1.48 (m, 2H), 1.48 – 1.42 (m, 1H), 1.42 – 1.32 (m, 2H). ^{13}C NMR (151 MHz, $CDCl_3$) δ 56.83, 54.04, 40.88, 39.56, 32.36, 30.79, 26.53.

2.7. General procedure D: the final step – *bis*-amide formation

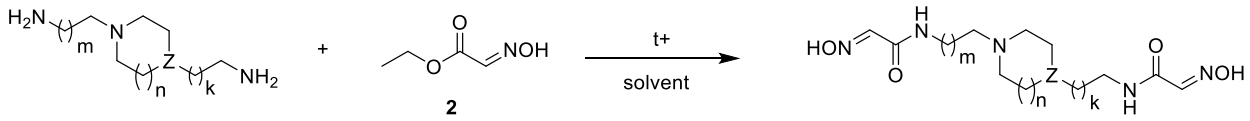

17 Z = N; n = 1; k = 1; m = 1
18 Z = N; n = 2; k = 1; m = 1
19 Z = N; n = 1; k = 1; m = 2
23 Z = N; n = 1; k = 2; m = 2
21 Z = N; n = 2; k = 2; m = 2
20 Z = C; n = 1; k = 1; m = 1
22 Z = C; n = 1; k = 1; m = 2

LG-700 Z = N; n = 1; k = 1; m = 1
LG-703 Z = N; n = 2; k = 1; m = 1
LG-750 Z = N; n = 1; k = 1; m = 2
LG-747 Z = N; n = 1; k = 2; m = 2
LG-804 Z = N; n = 2; k = 2; m = 2
LG-823 Z = C; n = 1; k = 1; m = 1
LG-829 Z = C; n = 1; k = 1; m = 2

The compound **17-23** (1.0 eq) and oxime-fragment **2** (2.5 eq) were dissolved in solvent (EtOH or MeCN, 3 mL) and heated (50–90 ˚C) for 1–3 days.

(2*E*)-2-(*N*-hydroxyimino)-*N*-[2-(4-{2-[(2*E*)-2-(*N*-hydroxyimino)acetamido]ethyl}piperazin-1-yl)ethyl]acetamide (LG-700): Prepared according to the general procedure D. Compound **17** (590 mg; 3.425 mmol) and oxime fragment **2** (1.003 g; 8.56 mmol) in EtOH (3 mL) as solvent was heated to 90 °C for 2 days. The solution was concentrated and directly purified by column chromatography using mobile phase DCM/MeOH (4:1). The result was precipitated in cold MeOH and filtered to give pure product **LG-700** as white solid. Yield 10%.

^{1}H NMR (600 MHz, DMSO-d_6) δ 11.94 (s, 2H), 7.95 (t, J = 5.8 Hz, 2H), 7.42 (s, 2H), 3.23 (q, J = 6.5 Hz, 4H), 2.36 (t, J = 6.8 Hz, 12H). ^{13}C NMR (151 MHz, DMSO-d_6) δ 162.08, 144.10, 57.09, 53.11, 36.29. HRMS (ESI$^+$): $[M+H]^+$: calculated for $C_{12}H_{23}N_6O_4^+$ (m/z): 315.1775; detected: 315.1772. LC-MS purity > 95%.

(2*E*)-2-(*N*-hydroxyimino)-*N*-[2-(4-{2-[(2*E*)-2-(*N*-hydroxyimino)acetamido]ethyl}-1,4-diazepan-1-yl)ethyl]acetamide (LG-703): Prepared according to the general procedure D. The compound **18** (305 mg; 1.64 mmol) and oxime fragment **2** (480 mg ; 4.1 mmol) in EtOH (3 mL) as solvent was heated to 90 °C for 3 days. The solution was concentrated and directly purified by column chromatography using mobile phase DCM/MeOH (2:1). The result was precipitated in cold MeOH and filtered to give pure product **LG-703** as white solid. Yield 19%.

^{1}H NMR (600 MHz, DMSO-d_6) δ 11.95 (s, 2H), 7.93 (t, J = 5.7 Hz, 2H), 7.41 (s, 2H), 3.20 (q, J = 6.5 Hz, 4H), 2.67 – 2.56 (m, 8H), 2.52 (t, J = 6.8 Hz, 4H), 1.65 (p, J = 5.8 Hz, 2H). ^{13}C NMR (151 MHz, DMSO-d_6) δ 162.09, 144.12, 56.50, 55.04, 54.01, 37.01, 27.69. HRMS

(ESI$^+$): [M+H]$^+$: calculated for $C_{13}H_{25}N_6O_4^+$ (m/z): 329.1932; detected: 329.1931. LC-MS purity > 98%.

(2*E*)-2-(*N*-hydroxyimino)-*N*-[3-(4-{2-[(2*E*)-2-(*N*-hydroxyimino)acetamido]ethyl}piperazin-1-yl)propyl]acetamide (LG-750): Prepared according to the general procedure D. Compound **19** (570 mg; 3.06 mmol) and oxime fragment **2** (896 mg; 7.65 mmol) in EtOH (3 mL) as solvent was heated to 90 °C for 2 days. The solution was concentrated and directly purified by column chromatography using mobile phase DCM/MeOH (2:1). The result was precipitated in cold MeOH and filtered to give pure product **LG-750** as white solid. Yield 14%.

^{1}H NMR (600 MHz, DMSO-d_6) δ 11.96 (s, 1H), 11.91 (s, 1H), 8.22 (t, *J* = 5.8 Hz, 1H), 7.98 (t, *J* = 5.8 Hz, 1H), 7.42 (s, 1H), 7.41 (s, 1H), 3.24 (q, *J* = 6.5 Hz, 2H), 3.14 (q, *J* = 6.5 Hz, 2H), 2.46 – 2.25 (m, 12H), 1.58 (p, *J* = 7.0 Hz, 2H). ^{13}C NMR (151 MHz, DMSO-d_6) δ 162.13, 144.20, 144.08, 56.98, 55.97, 37.53, 36.26, 26.34. HRMS (ESI$^+$): [M+H]$^+$: calculated for $C_{13}H_{25}N_6O_4^+$ (m/z): 329.1932; detected: 329.1933. LC-MS purity > 98%.

(2*E*)-2-(*N*-hydroxyimino)-*N*-[3-(4-{3-[(2*E*)-2-(*N*-hydroxyimino)acetamido]propyl}piperazin-1-yl)propyl]acetamide (LG-747): Prepared according to the general procedure D. Commercially available compound **23** (504 mg; 2.516 mmol) and oxime fragment **2** (737 mg; 6.29 mmol) in EtOH (3 mL) as solvent was heated to 90 °C for 3 days. The solution was concentrated and directly purified by column chromatography using mobile phase DCM/MeOH (2:1). The result was precipitated in cold MeOH and filtered to give pure product **LG-747** as white solid. Yield 13%.

^{1}H NMR (600 MHz, DMSO-d_6) δ 11.89 (s, 2H), 8.19 (s, 2H), 7.40 (s, 2H), 3.14 (q, *J* = 7.0 Hz, 4H), 2.50 – 2.49 (m, 4H), 2.25 (t, *J* = 7.0 Hz, 8H), 1.57 (p, *J* = 7.0 Hz, 4H). ^{13}C NMR (151 MHz, DMSO-d_6) δ 162.10, 144.22, 56.07, 37.61, 26.52. HRMS (ESI$^+$): [M+H]$^+$: calculated for $C_{14}H_{27}N_6O_4^+$ (m/z): 343.2088; detected: 343.2086. LC-MS purity > 97%.

(2*E*)-2-(*N*-hydroxyimino)-*N*-[3-(4-{3-[(2*E*)-2-(*N*-hydroxyimino)acetamido]propyl}-1,4-diazepan-1-yl)propyl]acetamide (LG-804): Prepared according to the general procedure D. Compound **21** (445 mg; 2.076 mmol) and oxime fragment **2** (608 mg; 5.19 mmol) in MeCN (3 mL) as solvent was heated to 50 °C for 2 days. The solution filtered and carefully washed by cold MeOH/EtOH (1:1) to give pure product **LG-804** as white solid. Yield 9%.

^{1}H NMR (600 MHz, DMSO-d_6) δ 8.21 (t, J = 6.0 Hz, 2H), 7.41 (s, 2H), 3.15 (q, J = 6.7 Hz, 4H), 2.60 – 2.53 (m, 8H), 2.41 (t, J = 7.2 Hz, 4H), 1.72 – 1.62 (m, 2H), 1.60 – 1.49 (m, 4H). ^{13}C NMR (151 MHz, DMSO) δ 162.10, 144.19, 144.18, 55.80, 55.02, 54.17, 37.60, 27.38, 27.26. HRMS (ESI$^+$): [M+H]$^+$: calculated for $C_{15}H_{29}N_6O_4^+$ (m/z): 357.2245; detected: 357.2242. LC-MS purity > 98%.

(2*E*)-2-(*N*-hydroxyimino)-*N*-[2-(1-{2-[(2*E*)-2-(*N*-hydroxyimino)acetamido]ethyl}piperidin-4-yl)ethyl]acetamide (LG-823): Prepared according to the general procedure D. Compound **20** (694 mg; 4.05 mmol) and oxime fragment **2** (1.186 g; 10.125 mmol) in EtOH (3 mL) as solvent was heated to 90 °C for 1 day. The solution was concentrated and directly purified by column chromatography using mobile phase DCM/MeOH (5:1) to give pure product **LG-823** as yellowish amorphous solid. Yield 13%.

^{1}H NMR (600 MHz, DMSO-d_6) δ 12.26 (s, 1H), 12.13 (s, 1H), 8.62 (t, J = 5.9 Hz, 1H), 8.43 (t, J = 6.0 Hz, 1H), 7.65 – 7.54 (m, 2H), 3.63 (q, J = 6.3 Hz, 2H), 3.51 – 3.40 (m, 2H), 3.35 – 3.25 (m, 2H), 3.16 – 3.06 (m, 2H), 2.91 – 2.76 (m, 2H), 1.99 – 1.87 (m, 2H), 1.62 – 1.48 (m, 5H). ^{13}C NMR (151 MHz, DMSO-d_6) δ 162.66, 162.19, 144.14, 143.83, 68.99, 56.20, 52.42, 45.74, 36.21, 34.38, 30.00. HRMS (ESI$^+$): [M+H]$^+$: calculated for $C_{13}H_{24}N_5O_4^+$ (m/z): 314.1823; detected: 314.1823. LC-MS purity > 95%.

(2*E*)-2-(*N*-hydroxyimino)-*N*-[3-(4-{2-[(2*E*)-2-(*N*-hydroxyimino)acetamido]ethyl}piperidin-1-yl)propyl]acetamide (LG-829): Prepared according to the general procedure D. Compound **22** (406 mg; 2.19 mmol) and oxime fragment **2** (513 mg; 5.475 mmol) in EtOH (3 mL) as solvent was heated to 90 °C for 3 days. The solution was concentrated and directly purified by column chromatography using mobile phase DCM/MeOH (4:1) to give pure product **LG-829** as yellowish amorphous solid. Yield 17%.

^{1}H NMR (600 MHz, DMSO-d_6) δ 12.13 – 11.81 (m, 2H), 8.23 (t, J = 5.8 Hz, 1H), 8.13 (t, J = 5.9 Hz, 1H), 7.42 (s, 1H), 7.41 (s, 1H), 3.16 – 3.12 (m, 4H), 2.89 – 2.75 (m, 2H), 2.27 (t, J = 7.1 Hz, 2H), 1.82 (t, J = 11.4 Hz, 2H), 1.67 – 1.51 (m, 4H), 1.36 (q, J = 7.1 Hz, 2H), 1.27 – 1.17 (m, 1H), 1.14 – 1.10 (m, 2H). ^{13}C NMR (151 MHz, DMSO-d_6) δ 162.13, 162.07, 144.19, 144.18, 68.97, 56.40, 56.22, 53.75, 37.68, 36.49, 36.08, 32.01, 30.01, 26.46. HRMS (ESI$^+$):

$[M+H]^+$: calculated for $C_{14}H_{26}N_5O_4^+$ (m/z): 328.1979; detected: 328.1975. LC-MS purity > 95 %.

3. NMR; HRMS and HPLC spectrums

(2*E*)-2-(*N*-hydroxyimino)-*N*-[2-(4-{2-[(2*E*)-2-(*N*-hydroxyimino)acetamido]ethyl}piperazin-1-yl)ethyl]acetamide (LG-700) ^{1}H NMR:

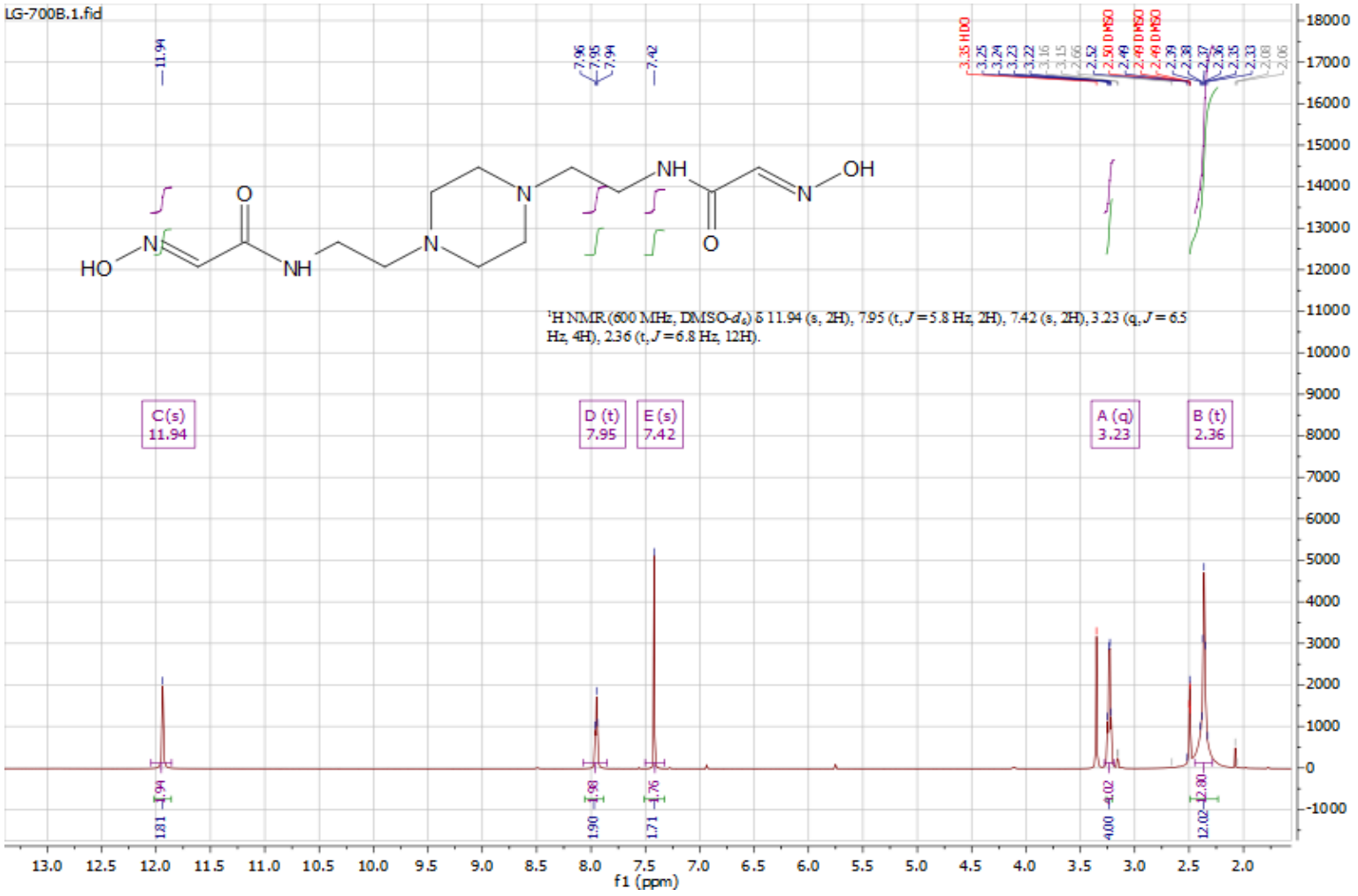

(2*E*)-2-(N-hydroxyimino)-*N*-[2-(4-{2-[(2*E*)-2-(*N*-hydroxyimino)acetamido]ethyl}piperazin-1-yl)ethyl]acetamide (LG-700) ^{13}C NMR:

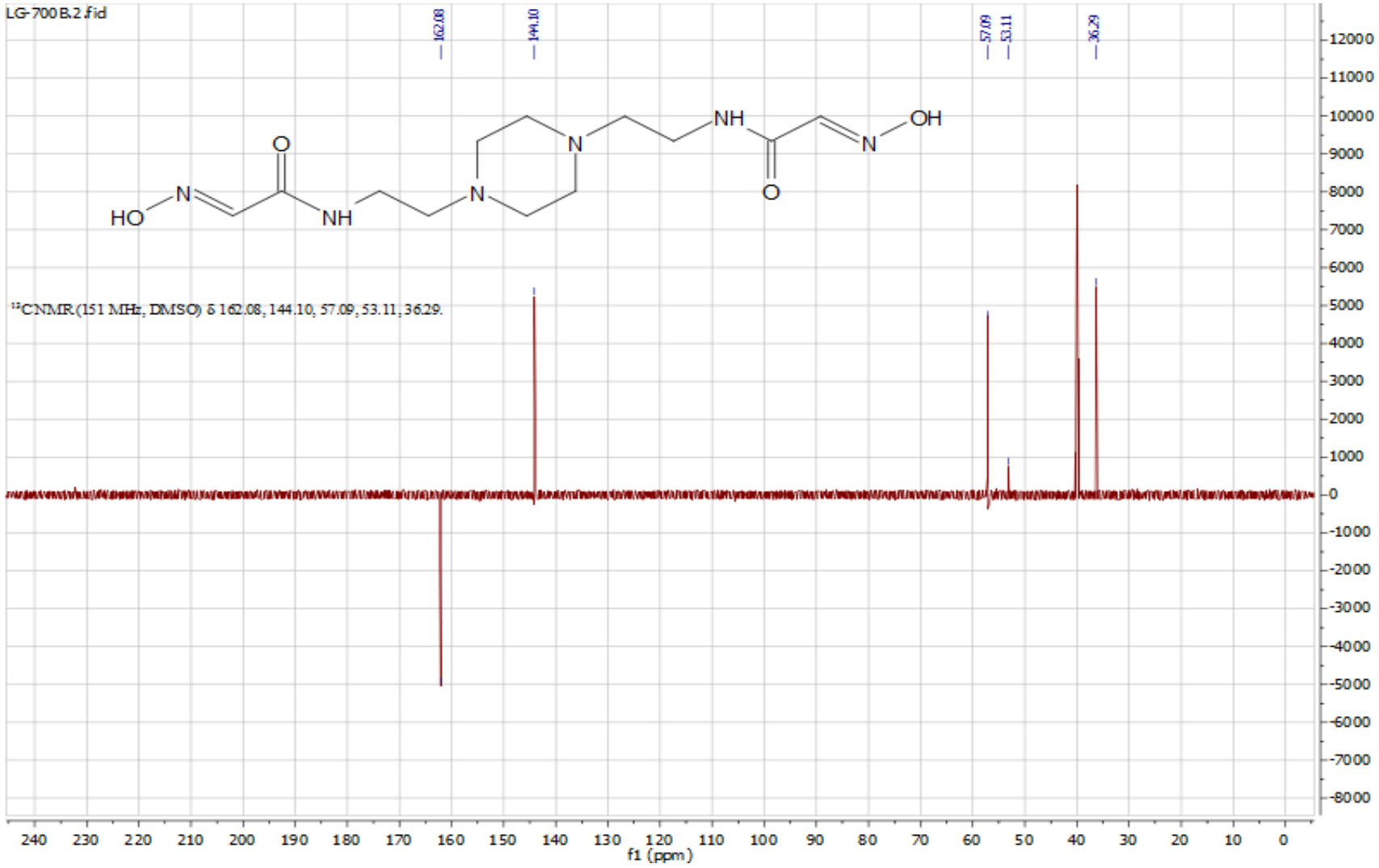

(2*E*)-2-(*N*-hydroxyimino)-*N*-[2-(4-{2-[(2*E*)-2-(*N*-hydroxyimino)acetamido]ethyl}-1,4-diazepan-1-yl)ethyl]acetamide (LG-703) ^{1}H NMR:

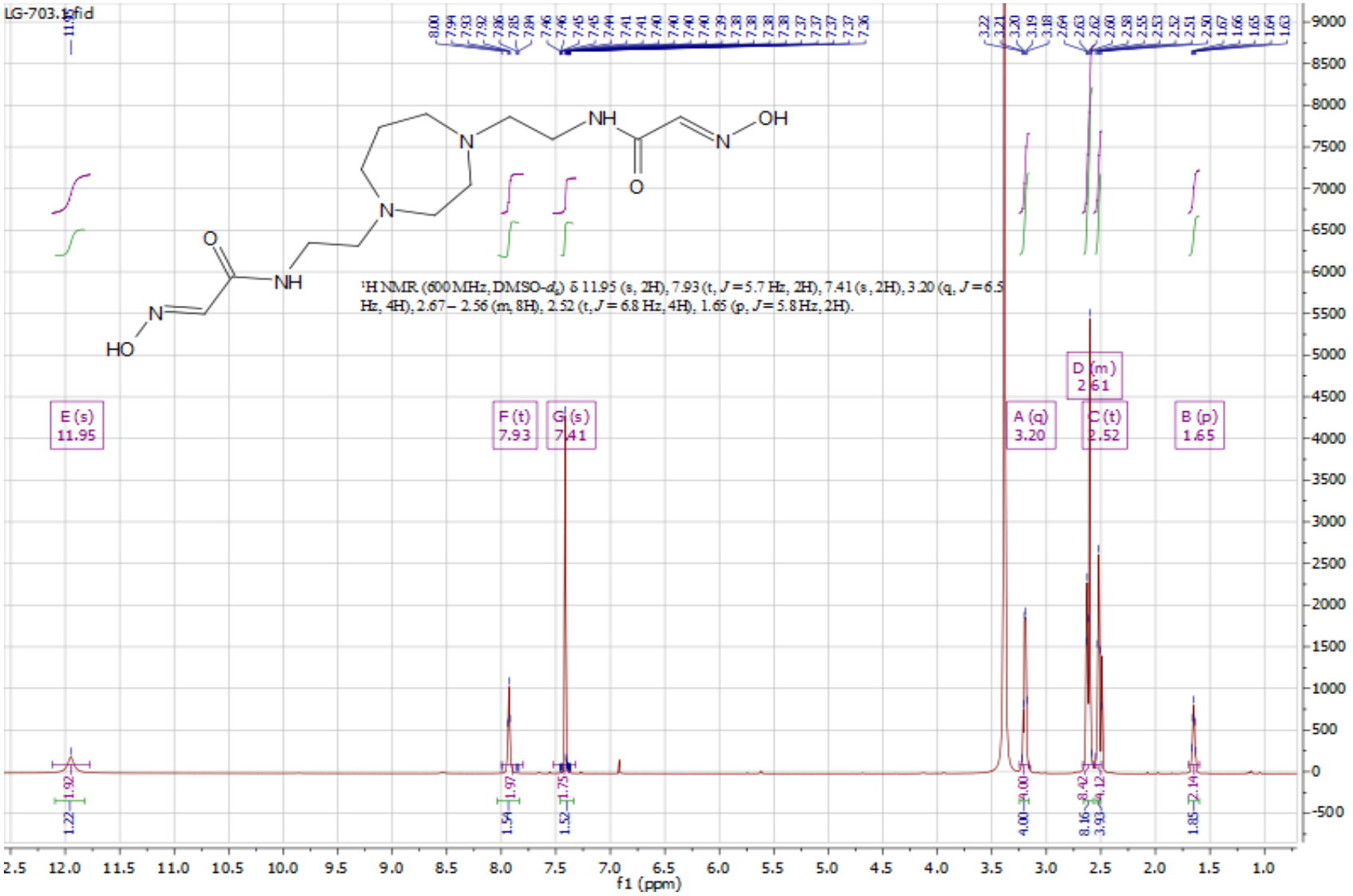

(2*E*)-2-(*N*-hydroxyimino)-*N*-[2-(4-{2-[(2*E*)-2-(*N*-hydroxyimino)acetamido]ethyl}-1,4-diazepan-1-yl)ethyl]acetamide (LG-703) ^{13}C NMR:

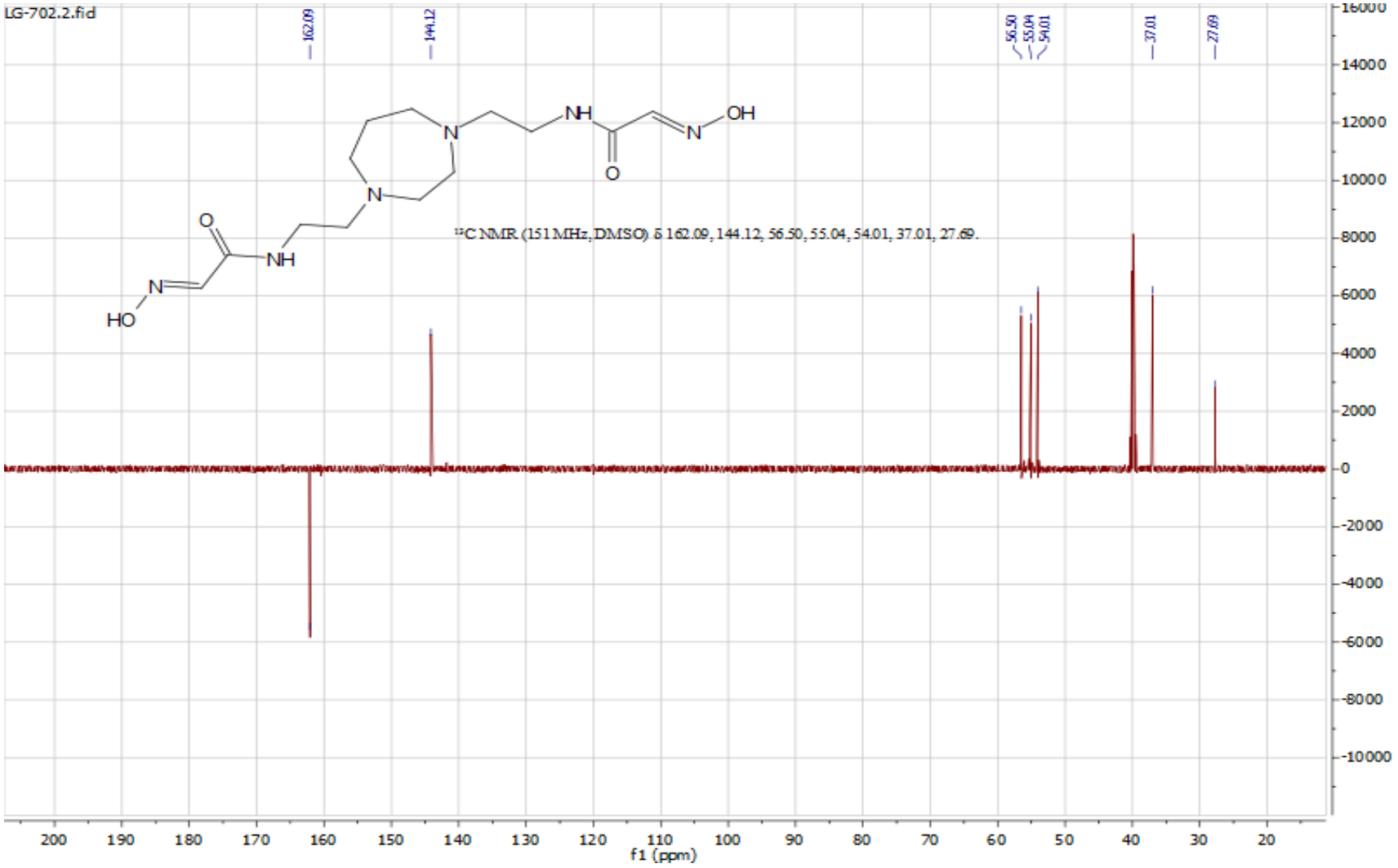

(2*E*)-2-(*N*-hydroxyimino)-*N*-[3-(4-{2-[(2*E*)-2-(*N*-hydroxyimino)acetamido]ethyl}piperazin-1-yl)propyl]acetamide (LG-750) ^{1}H NMR:

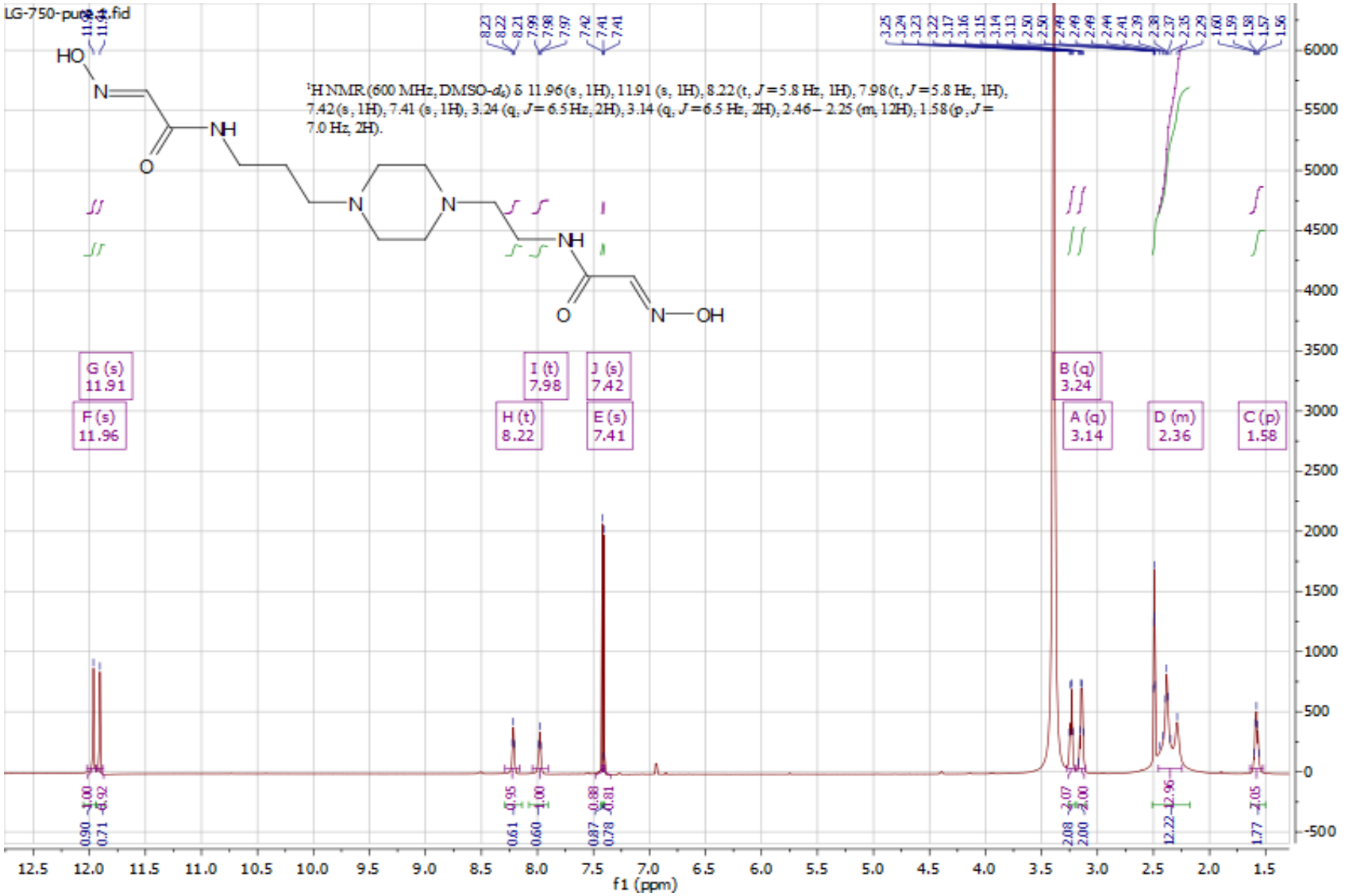

(2*E*)-2-(*N*-hydroxyimino)-*N*-[3-(4-{2-[(2*E*)-2-(*N*-hydroxyimino)acetamido]ethyl}piperazin-1-yl)propyl]acetamide (LG-750) ^{13}C NMR:

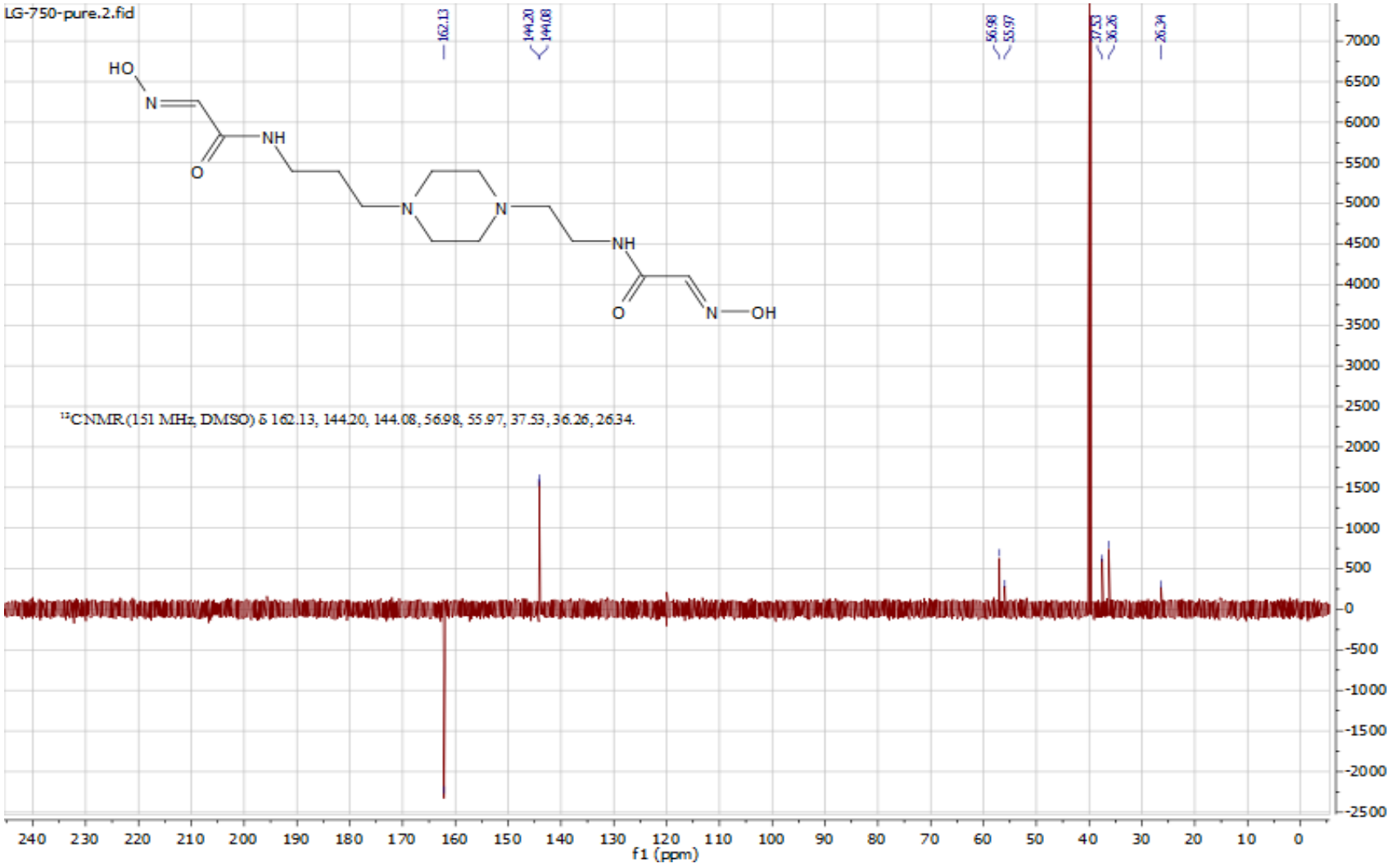

(2*E*)-2-(*N*-hydroxyimino)-*N*-[3-(4-{3-[(2*E*)-2-(*N*-hydroxyimino)acetamido]propyl}piperazin-1-yl)propyl]acetamide (LG-747) ^{1}H NMR:

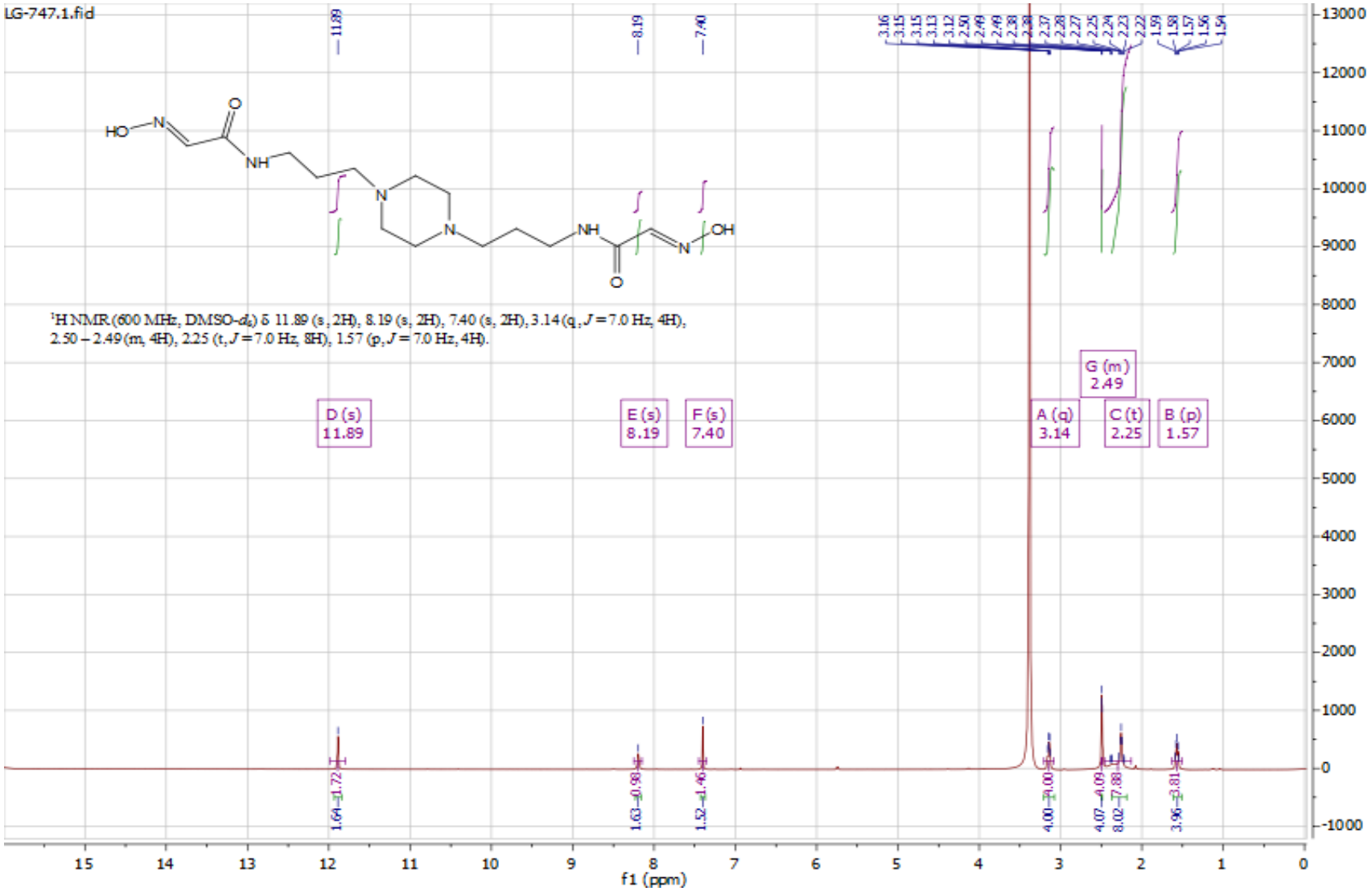

(2*E*)-2-(*N*-hydroxyimino)-*N*-[3-(4-{3-[(2*E*)-2-(*N*-hydroxyimino)acetamido]propyl}piperazin-1-yl)propyl]acetamide (LG-747) ^{13}C NMR:

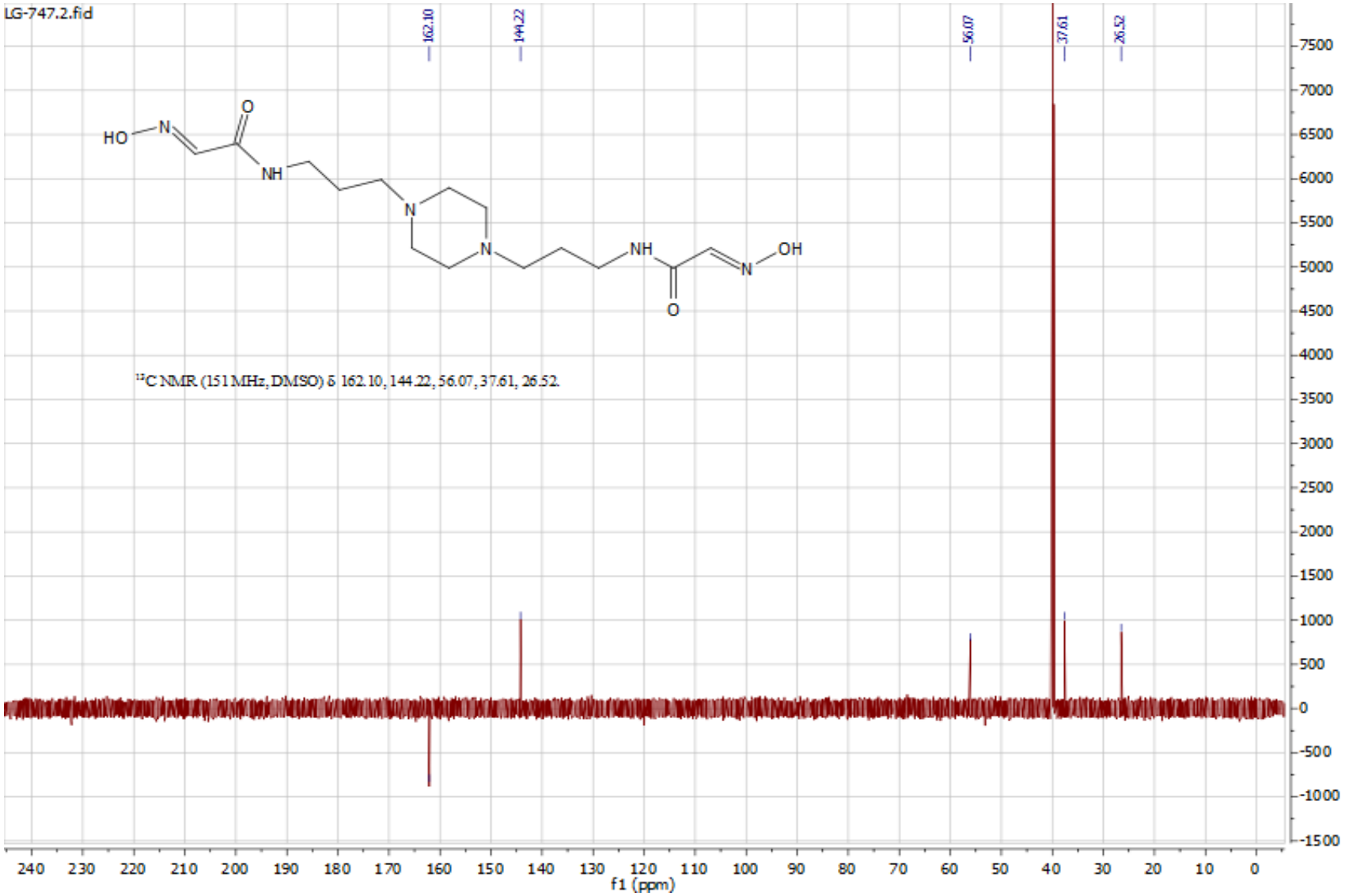

(2*E*)-2-(N-hydroxyimino)-*N*-[3-(4-{3-[(2*E*)-2-(*N*-hydroxyimino)acetamido]propyl}-1,4-diazepan-1-yl)propyl]acetamide (LG-804) ^{1}H NMR:

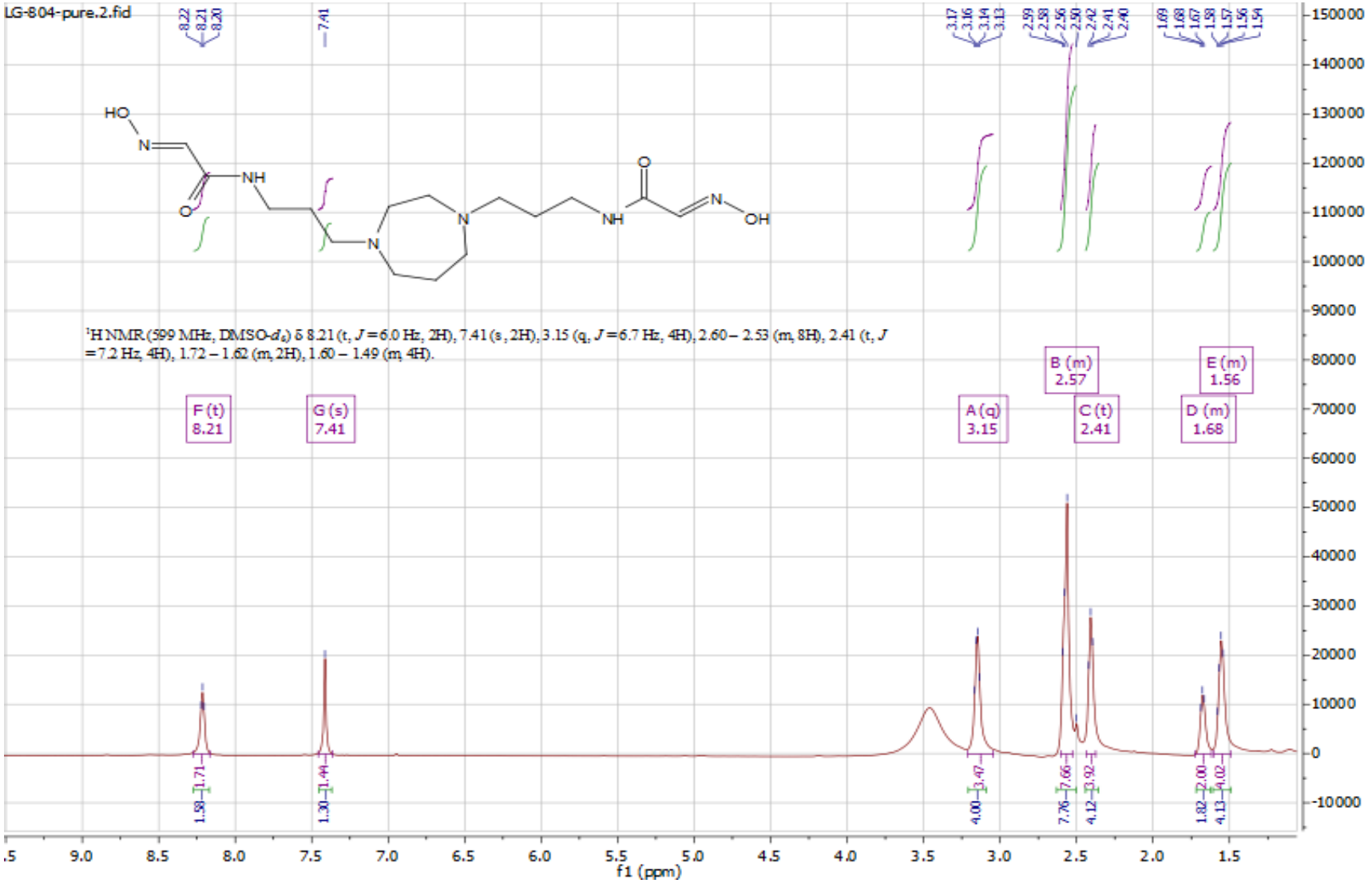

(2*E*)-2-(*N*-hydroxyimino)-*N*-[3-(4-{3-[(2*E*)-2-(*N*-hydroxyimino)acetamido]propyl}-1,4-diazepan-1-yl)propyl]acetamide (LG-804) ^{13}C NMR:

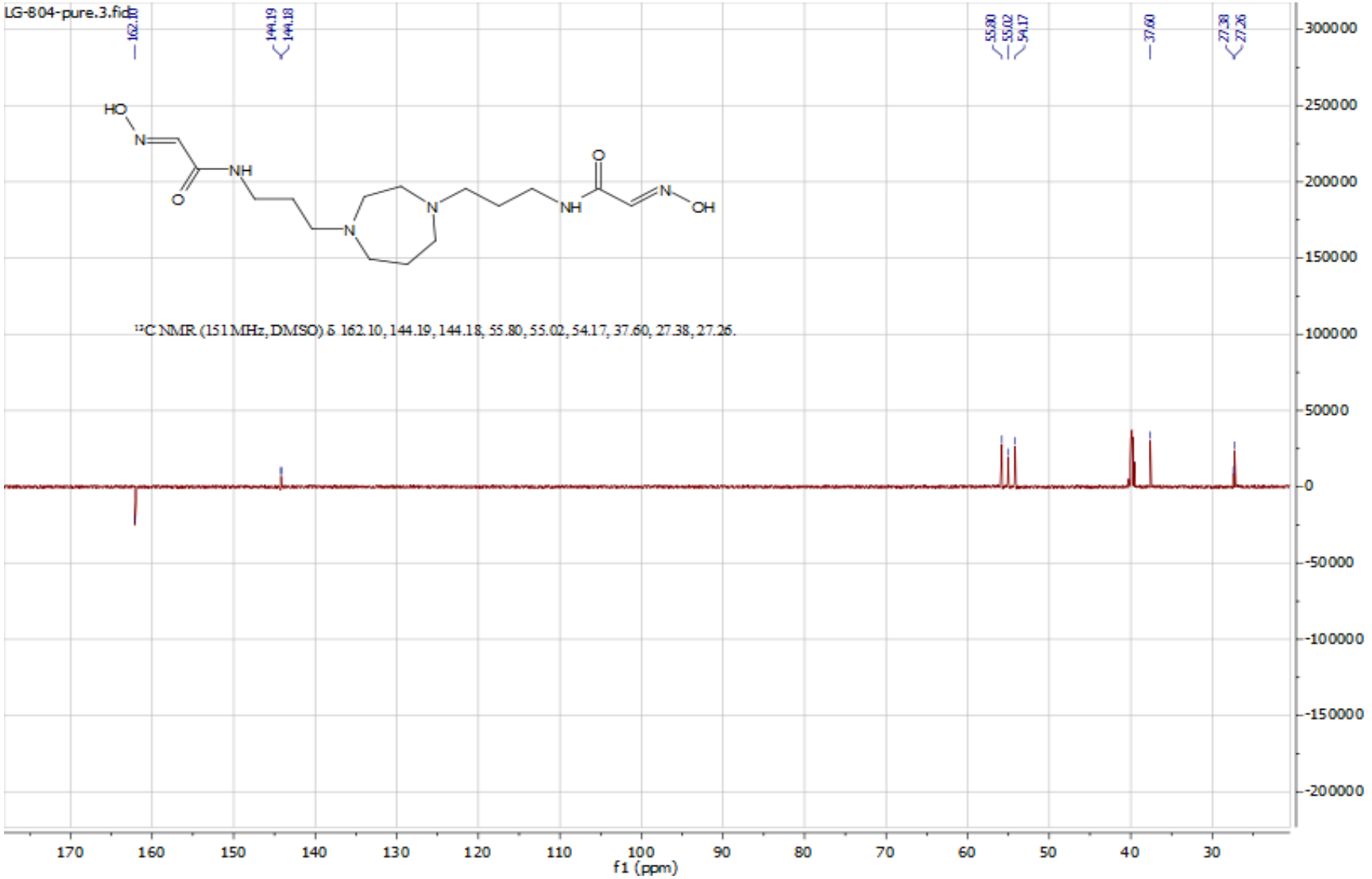

(2*E*)-2-(*N*-hydroxyimino)-*N*-[2-(1-{2-[(2*E*)-2-(*N*-hydroxyimino)acetamido]ethyl}piperidin-4-yl)ethyl]acetamide (LG-823) ^{1}H NMR:

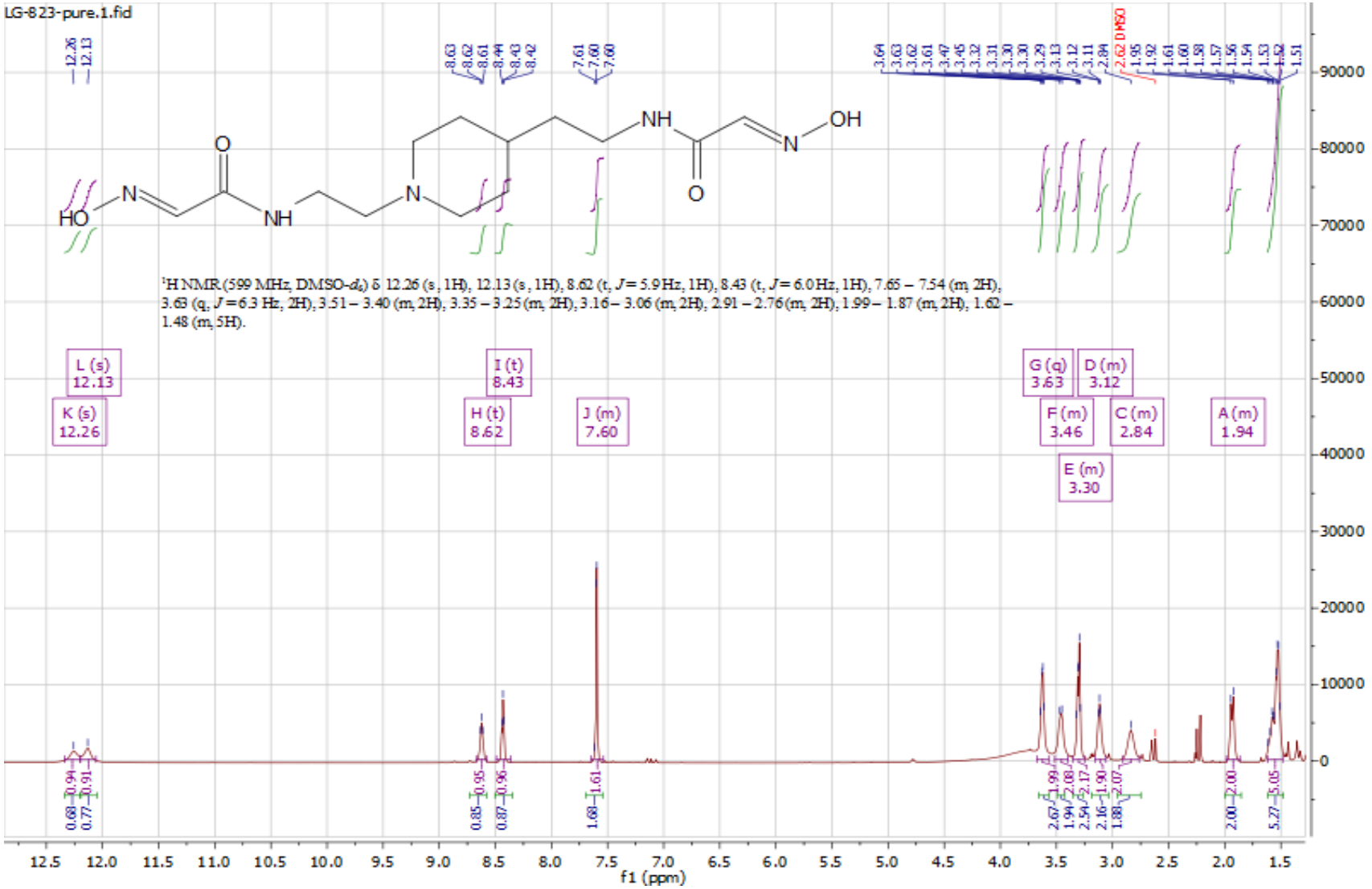

(2*E*)-2-(*N*-hydroxyimino)-*N*-[2-(1-{2-[(2*E*)-2-(*N*-hydroxyimino)acetamido]ethyl}piperidin-4-yl)ethyl]acetamide (LG-823) ^{13}C NMR:

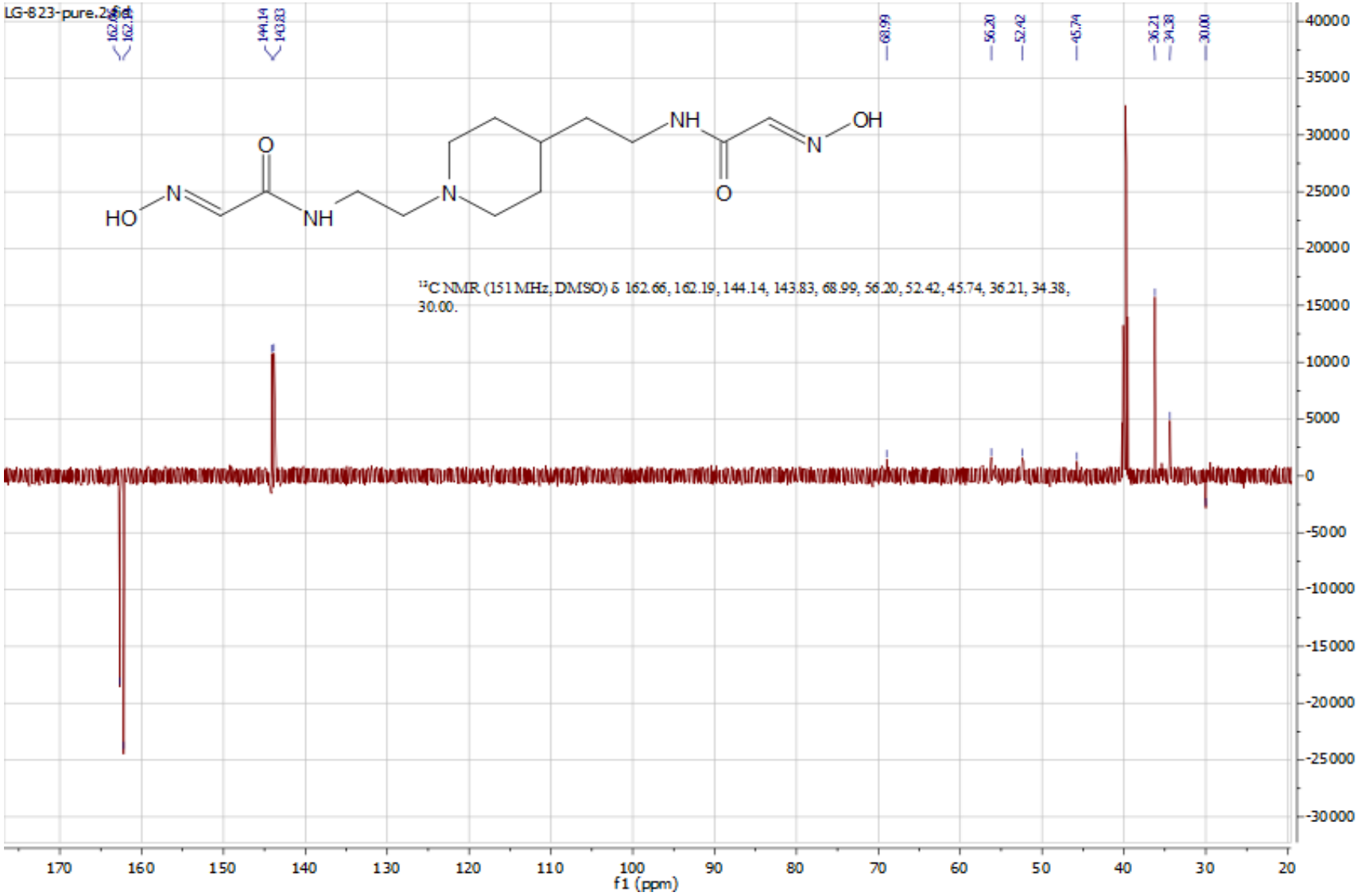

(2*E*)-2-(*N*-hydroxyimino)-*N*-[3-(4-{2-[(2*E*)-2-(*N*-hydroxyimino)acetamido]ethyl}piperidin-1-yl)propyl]acetamide (LG-829) ^{1}H NMR:

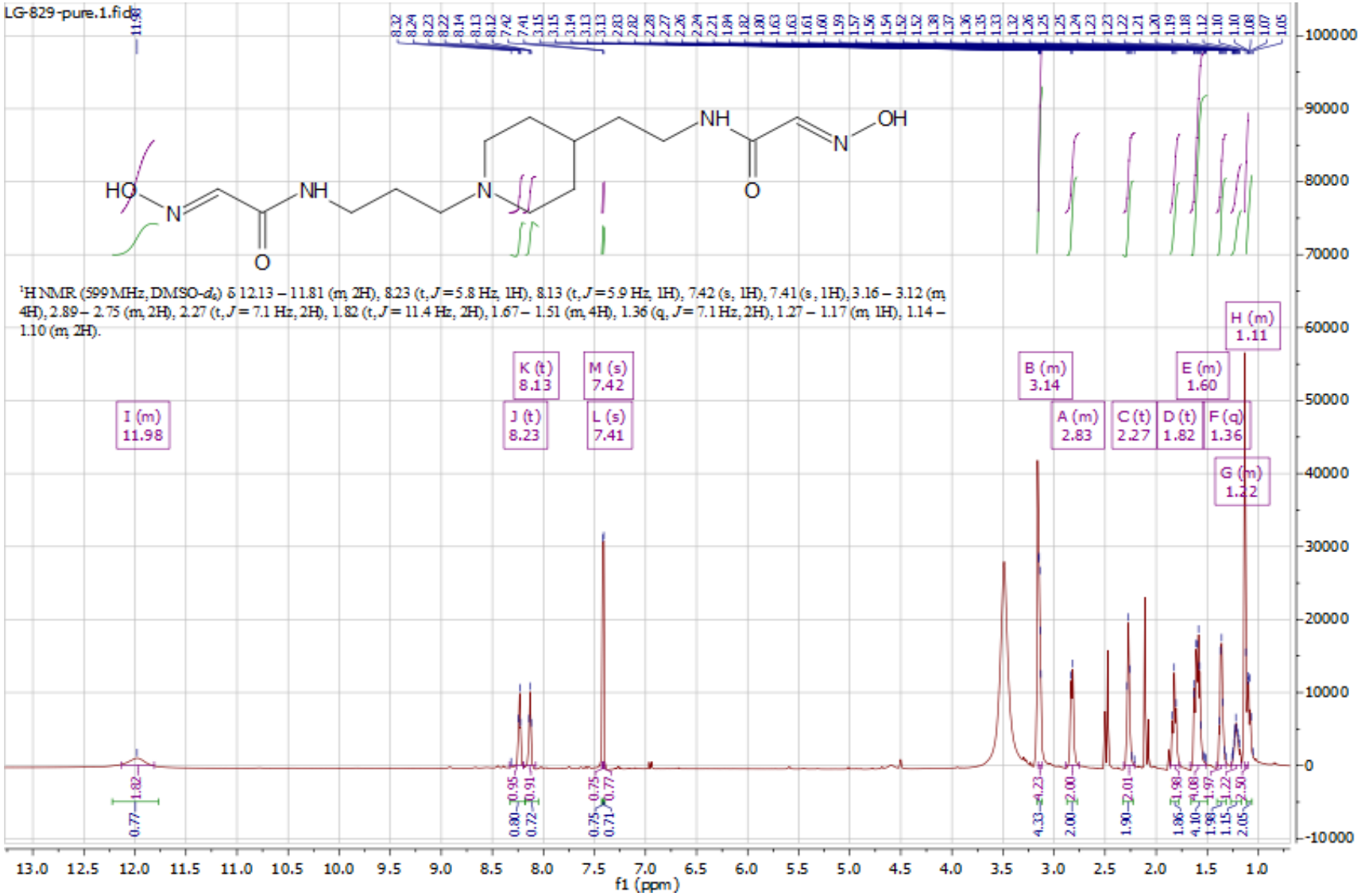

(2*E*)-2-(*N*-hydroxyimino)-*N*-[3-(4-{2-[(2*E*)-2-(*N*-hydroxyimino)acetamido]ethyl}piperidin-1-yl)propyl]acetamide (LG-829) ^{13}C NMR:

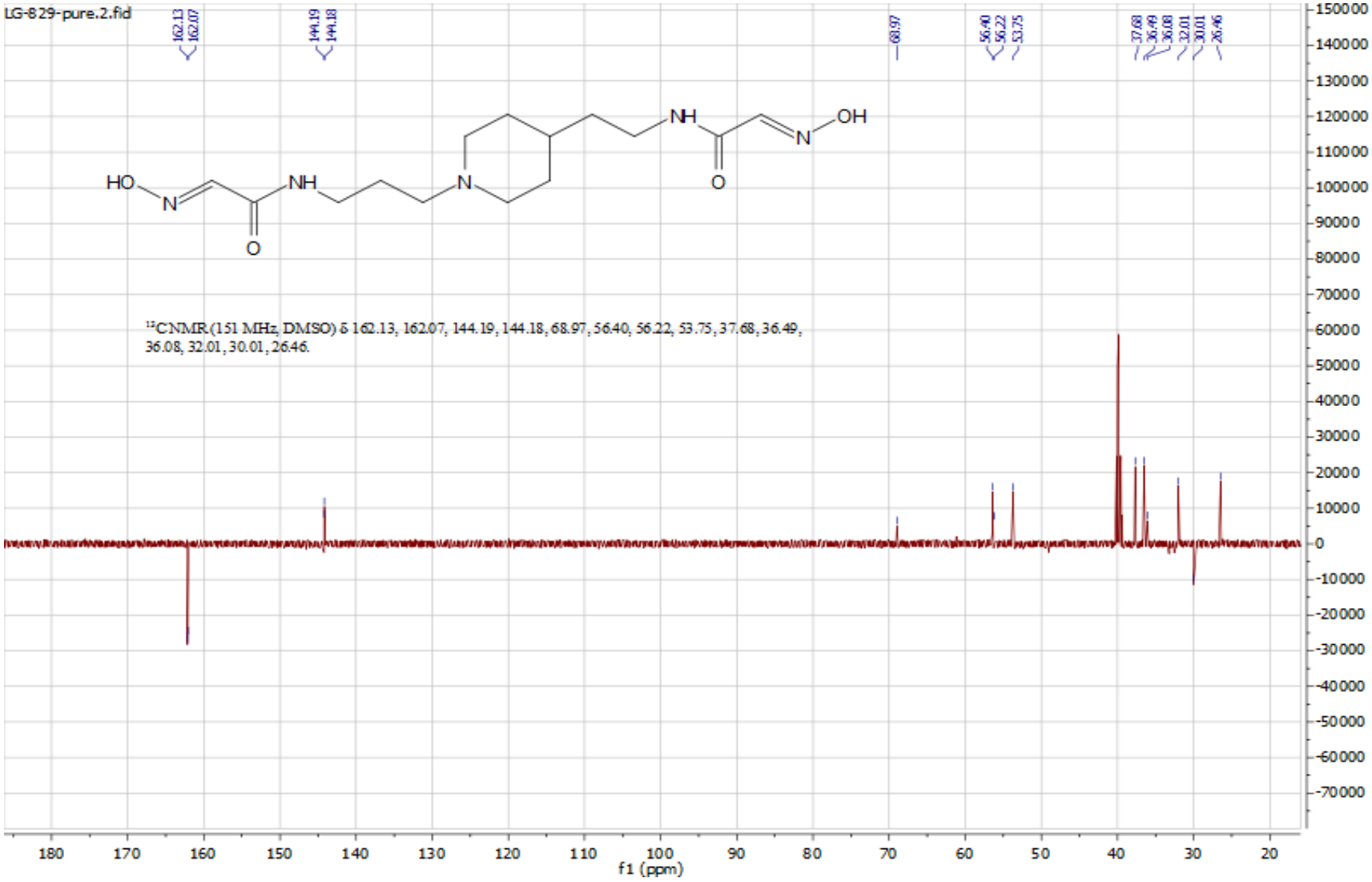

(2*E*)-2-(*N*-hydroxyimino)-*N*-[2-(4-{2-[(2*E*)-2-(*N*-hydroxyimino)acetamido]ethyl}piperazin-1-yl)ethyl]acetamide (LG-700) HRMS:

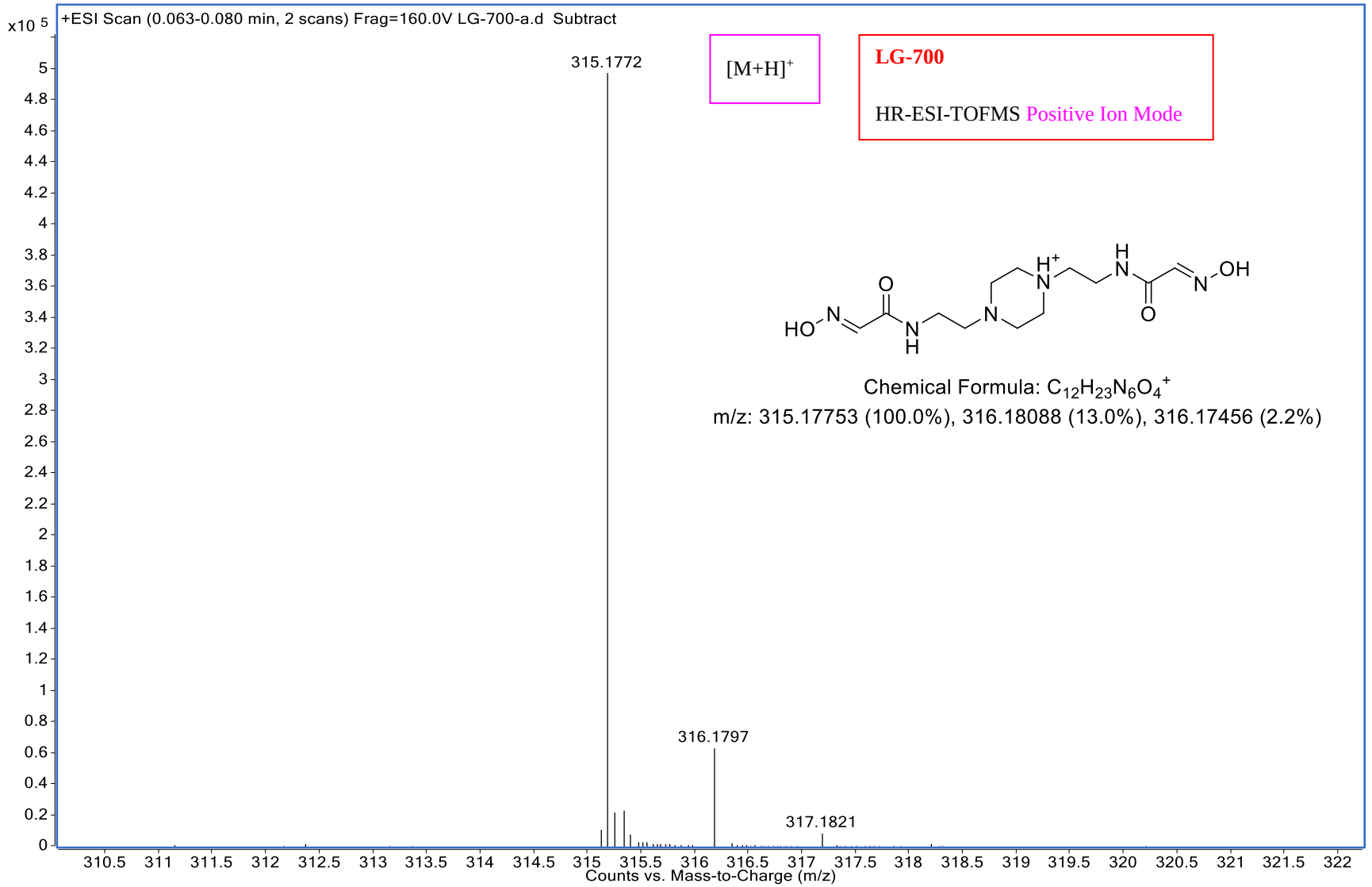

(2*E*)-2-(*N*-hydroxyimino)-*N*-[2-(4-{2-[(2*E*)-2-(*N*-hydroxyimino)acetamido]ethyl}-1,4-diazepan-1-yl)ethyl]acetamide (LG-703) HRMS:

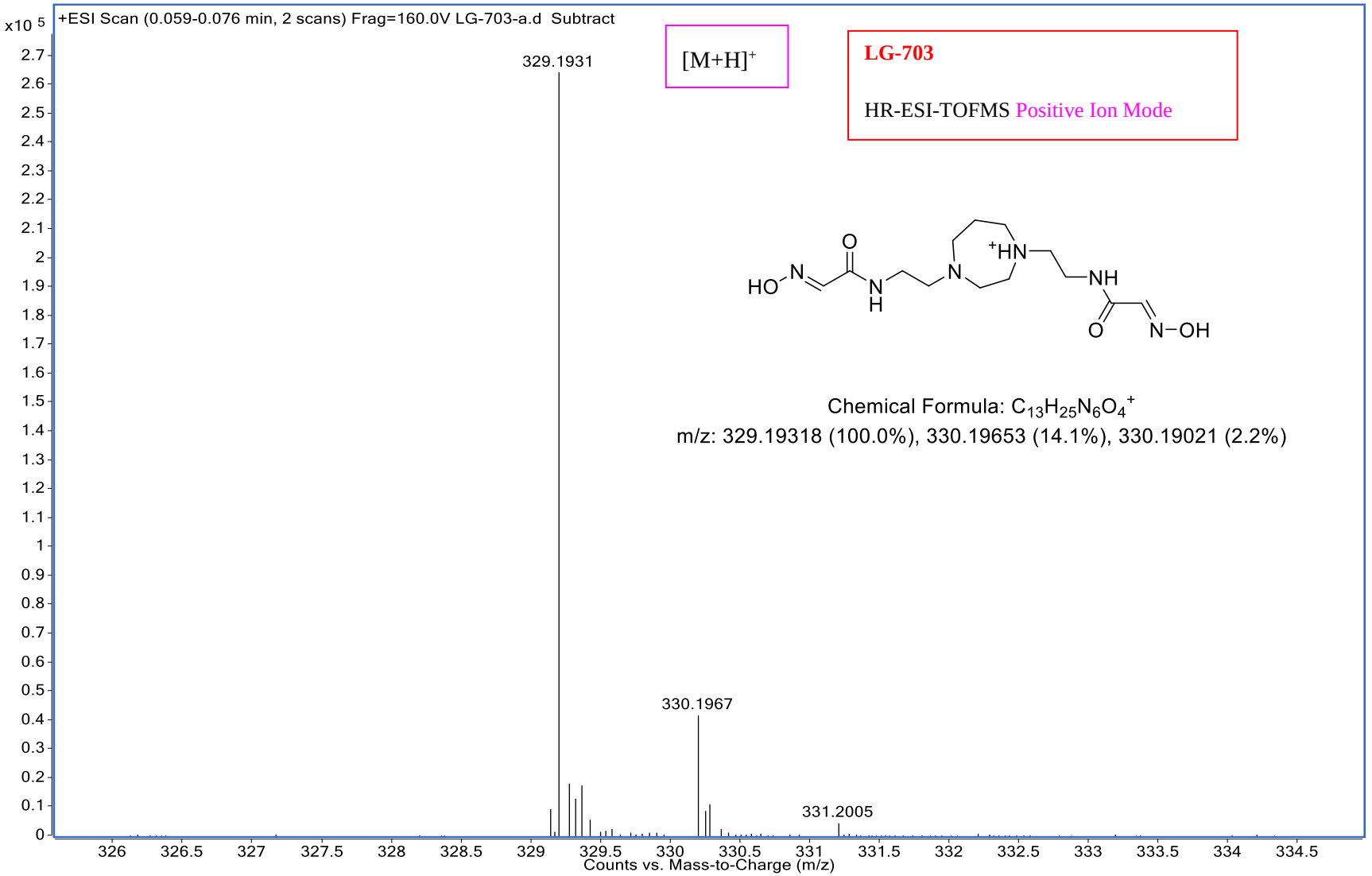

(2*E*)-2-(*N*-hydroxyimino)-*N*-[3-(4-{2-[(2*E*)-2-(*N*-hydroxyimino)acetamido]ethyl}piperazin-1-yl)propyl]acetamide (LG-750) HRMS:

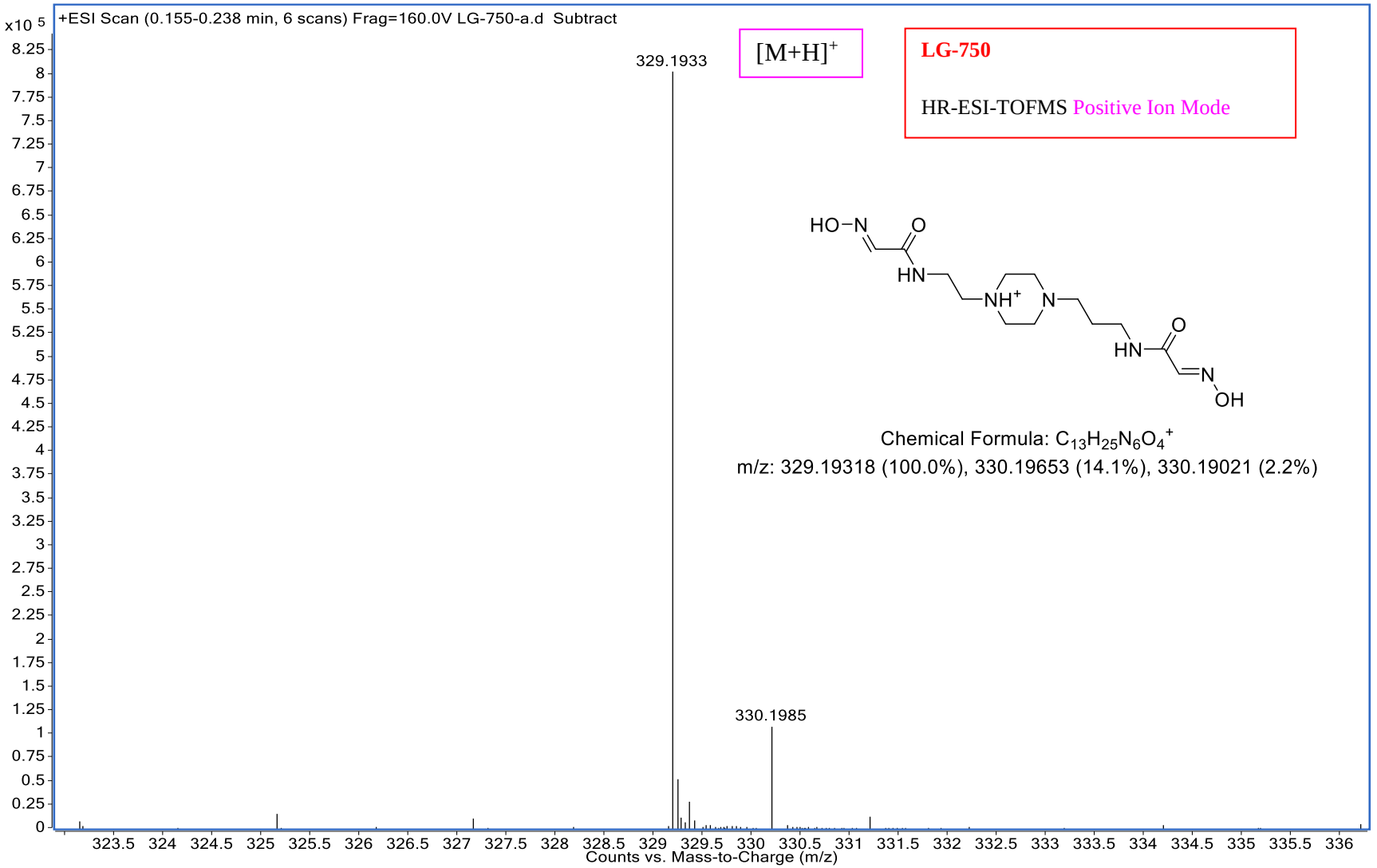

(2*E*)-2-(*N*-hydroxyimino)-*N*-[3-(4-{3-[(2*E*)-2-(*N*-hydroxyimino)acetamido]propyl}piperazin-1-yl)propyl]acetamide (LG-747) HRMS:

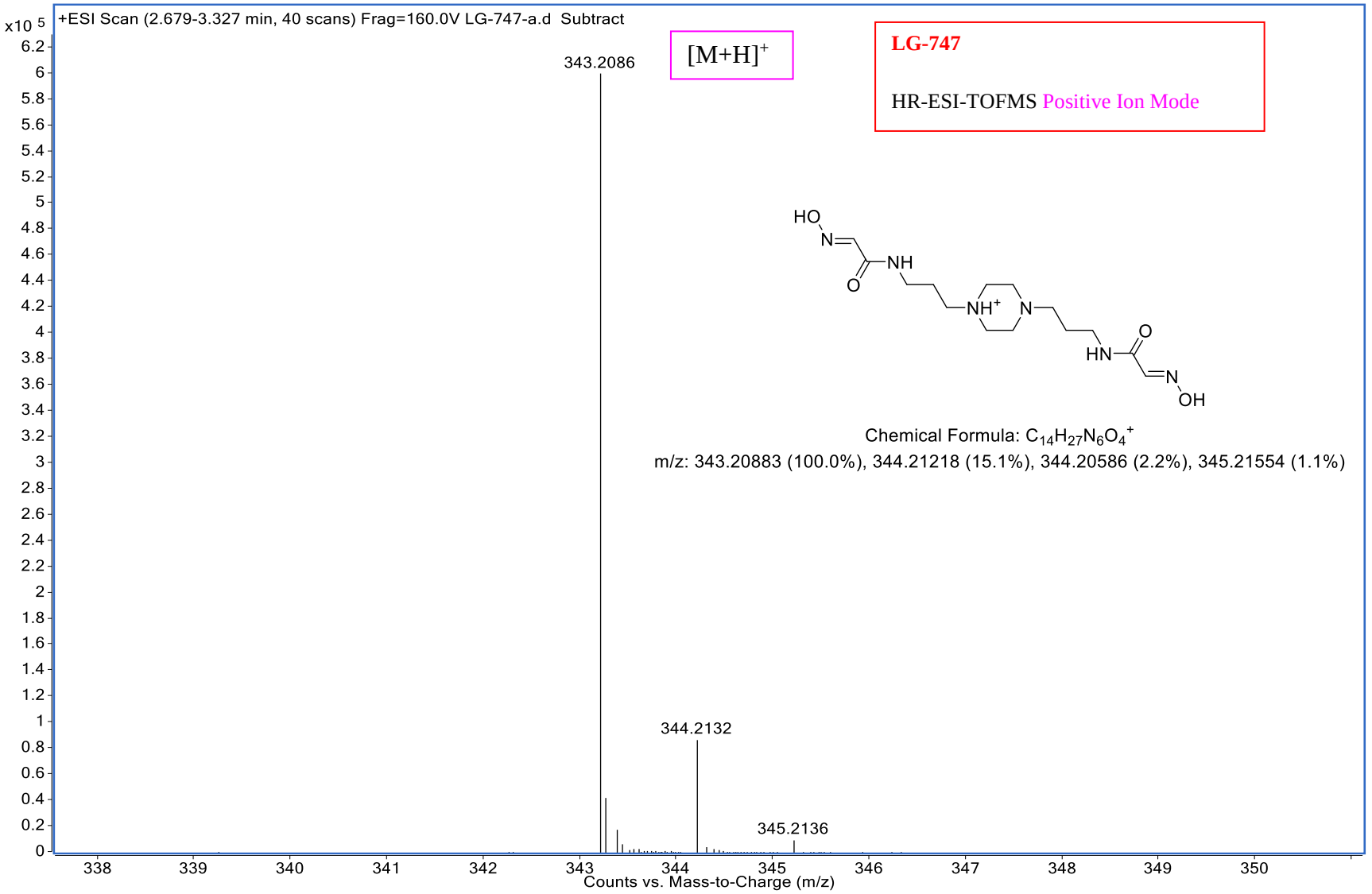

(2*E*)-2-(*N*-hydroxyimino)-*N*-[3-(4-{3-[(2*E*)-2-(*N*-hydroxyimino)acetamido]propyl}-1,4-diazepan-1-yl)propyl]acetamide (LG-804) HRMS:

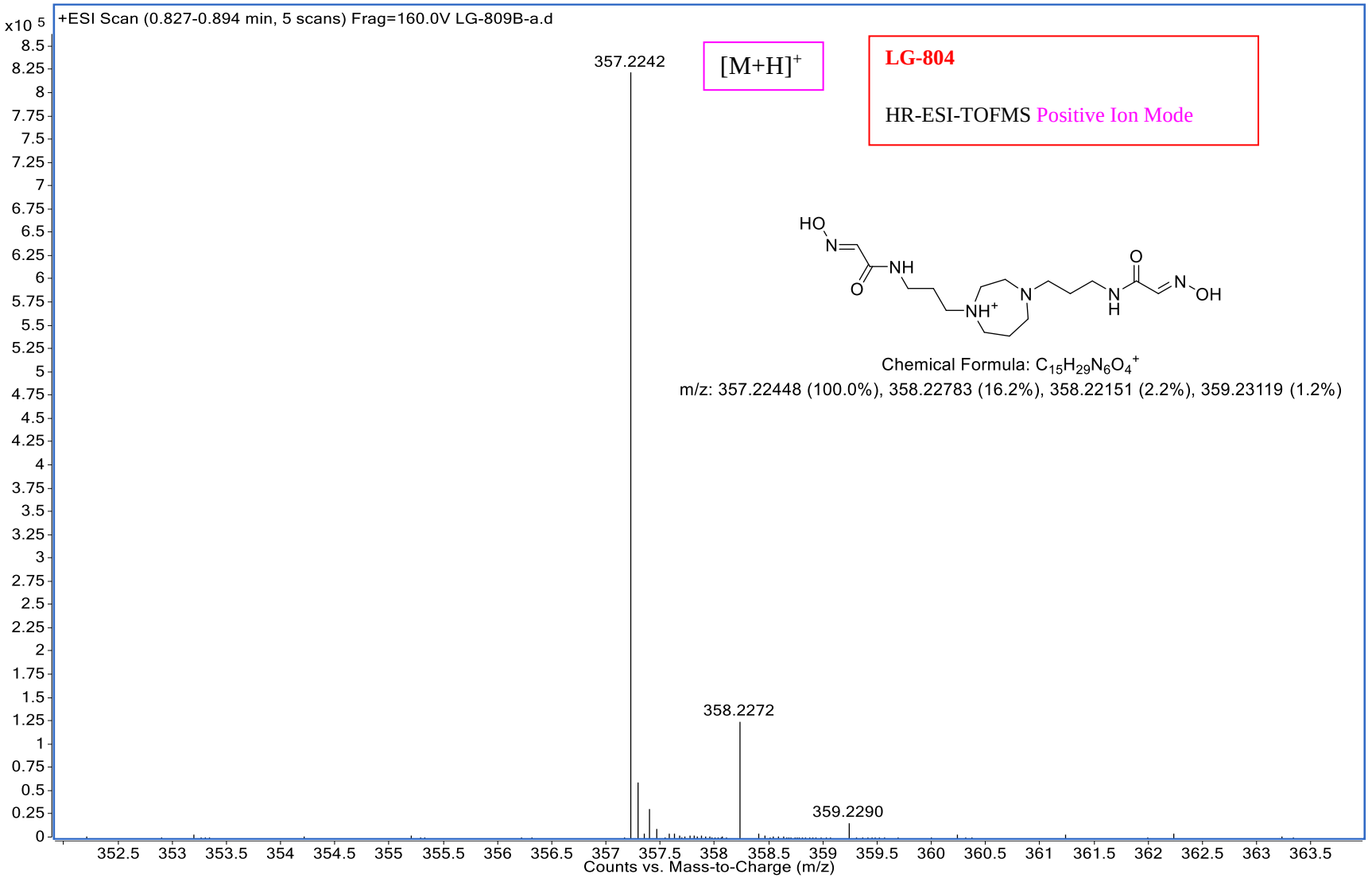

(2*E*)-2-(*N*-hydroxyimino)-*N*-[2-(1-{2-[(2*E*)-2-(*N*-hydroxyimino)acetamido]ethyl}piperidin-4-yl)ethyl]acetamide (LG-823) HRMS:

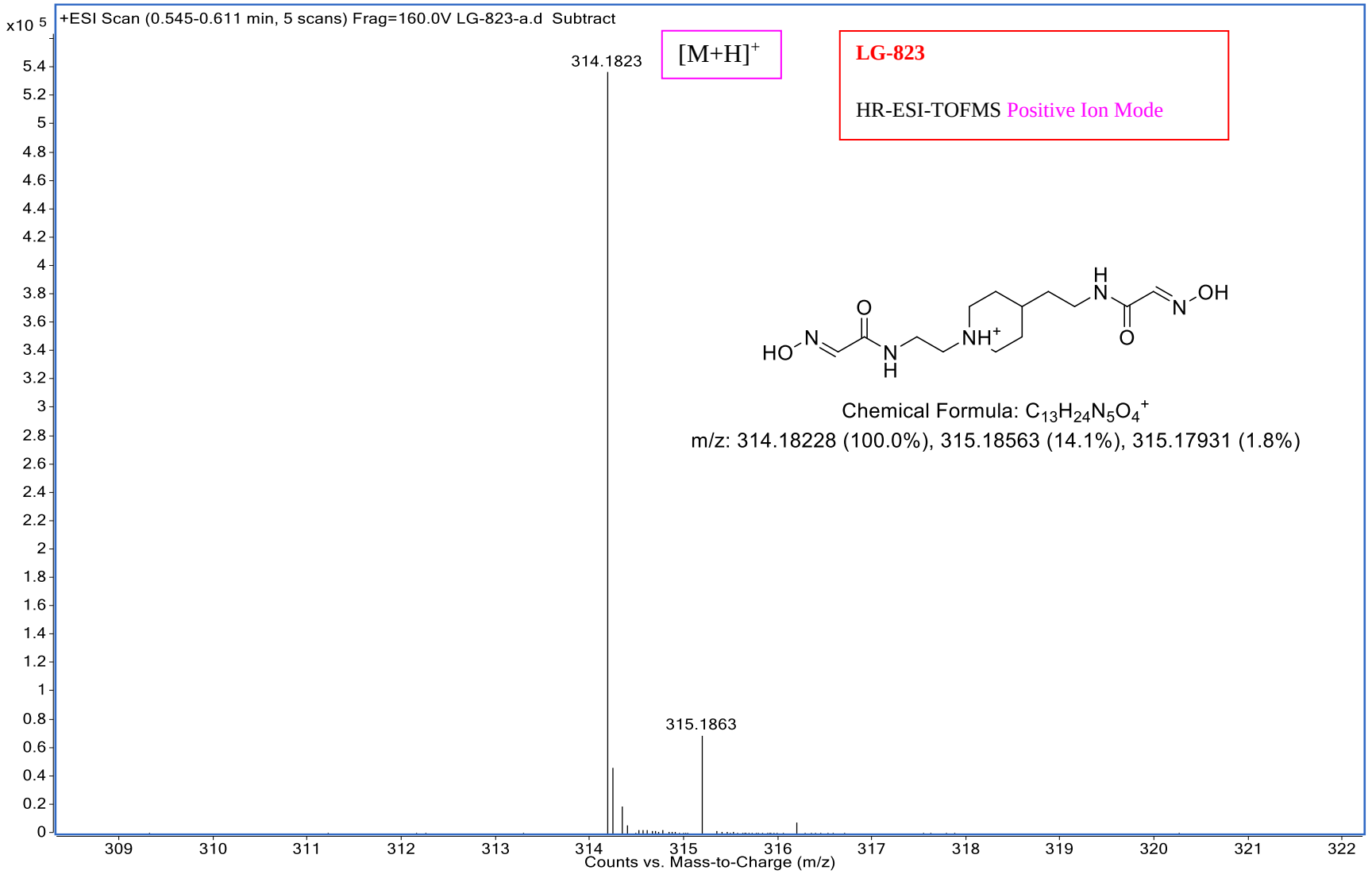

(2*E*)-2-(*N*-hydroxyimino)-*N*-[3-(4-{2-[(2*E*)-2-(*N*-hydroxyimino)acetamido]ethyl}piperidin-1-yl)propyl]acetamide (LG-829) HRMS:

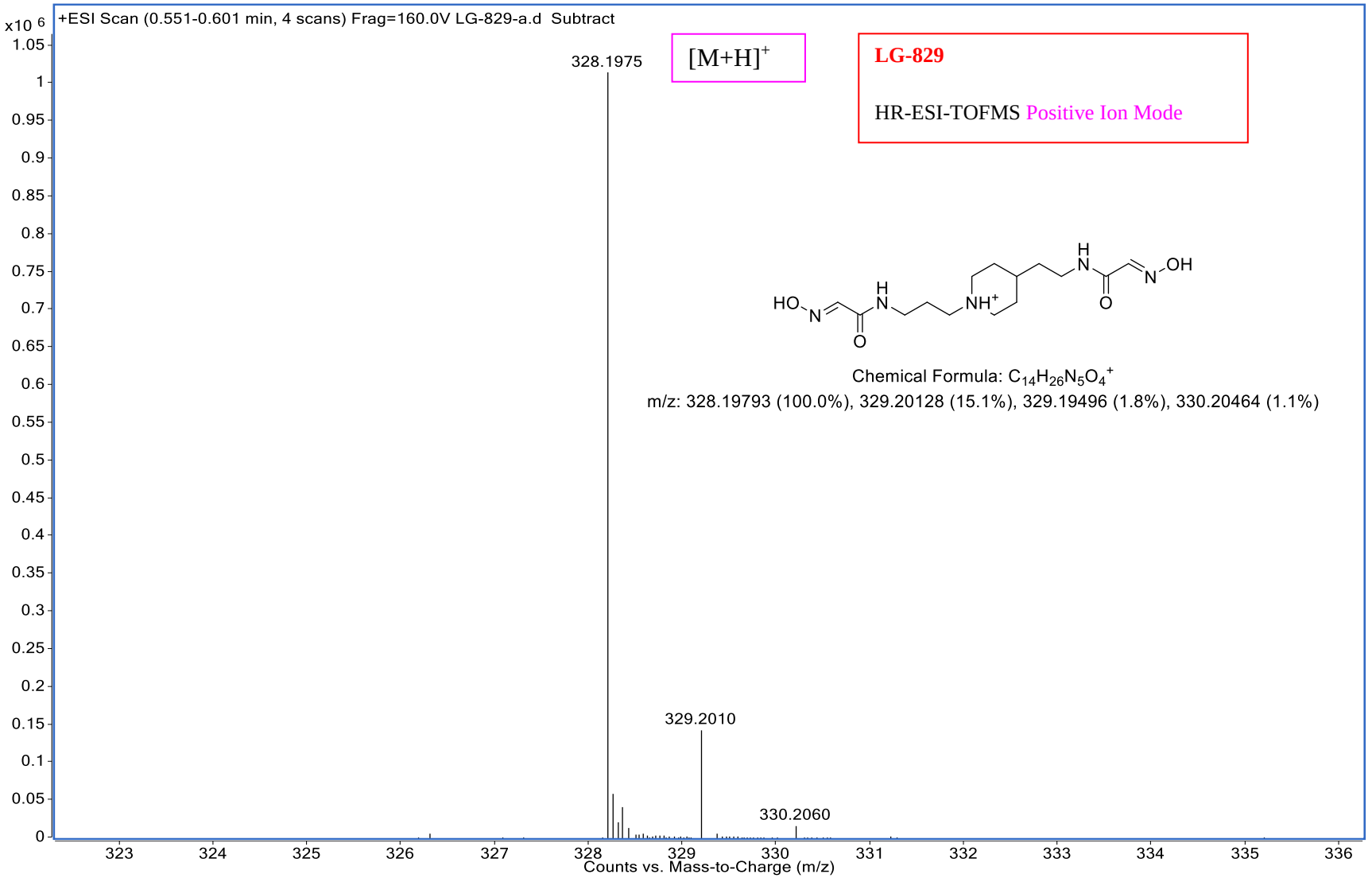

(2*E*)-2-(*N*-hydroxyimino)-*N*-[2-(4-{2-[(2*E*)-2-(*N*-hydroxyimino)acetamido]ethyl}piperazin-1-yl)ethyl]acetamide (LG-700) LC-MS purity:

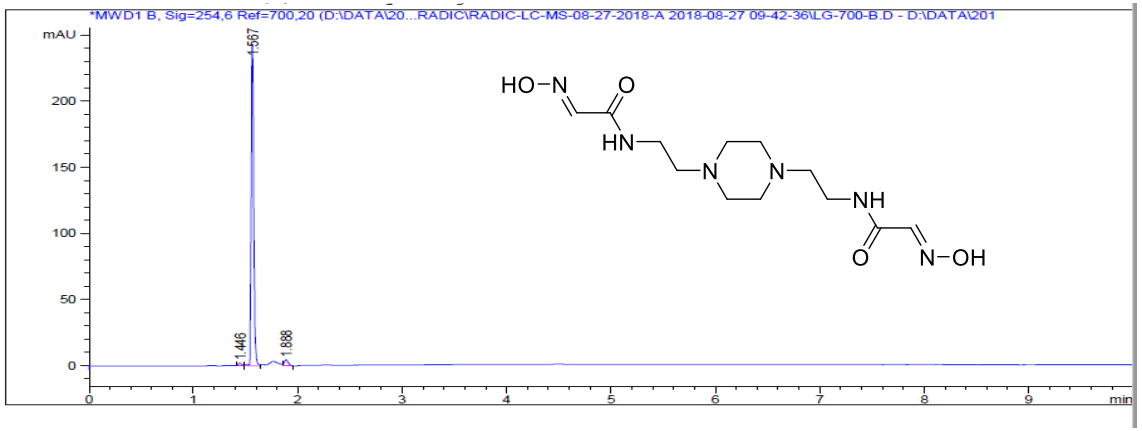

(2*E*)-2-(*N*-hydroxyimino)-*N*-[2-(4-{2-[(2*E*)-2-(*N*-hydroxyimino)acetamido]ethyl}-1,4-diazepan-1-yl)ethyl]acetamide (LG-703) LC-MS purity:

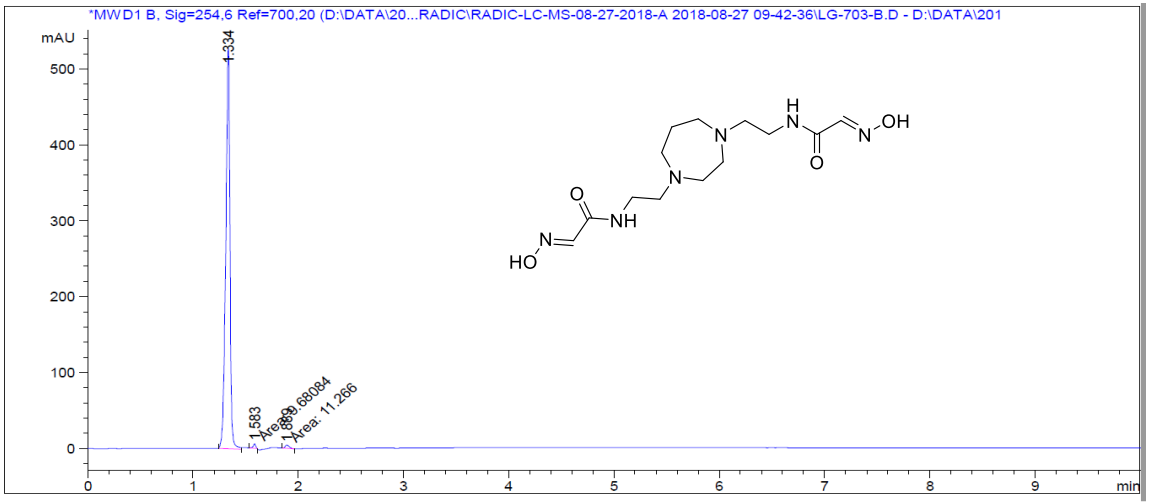

(2*E*)-2-(*N*-hydroxyimino)-*N*-[3-(4-{2-[(2*E*)-2-(*N*-hydroxyimino)acetamido]ethyl}piperazin-1-yl)propyl]acetamide (LG-750) LC-MS purity:

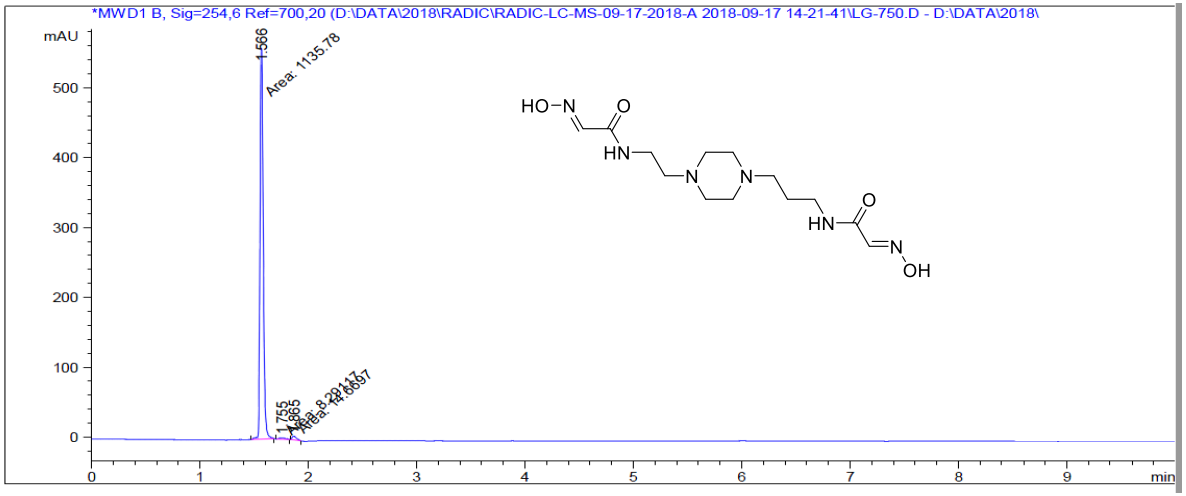

(2*E*)-2-(*N*-hydroxyimino)-*N*-[3-(4-{3-[(2*E*)-2-(*N*-hydroxyimino)acetamido]propyl}piperazin-1-yl)propyl]acetamide (LG-747) LC-MS purity:

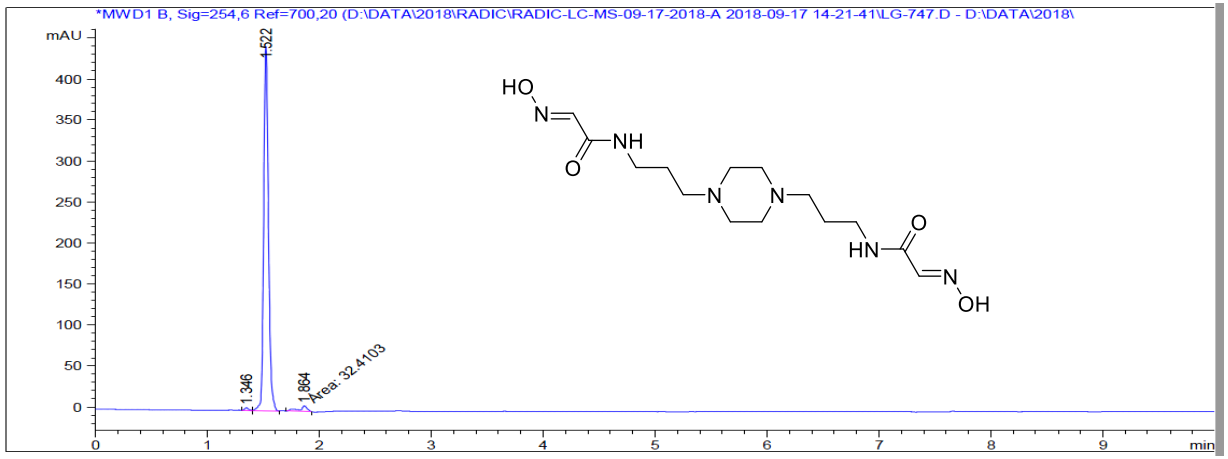

(2*E*)-2-(*N*-hydroxyimino)-*N*-[3-(4-{3-[(2*E*)-2-(*N*-hydroxyimino)acetamido]propyl}-1,4-diazepan-1-yl)propyl]acetamide (LG-804) LC-MS purity:

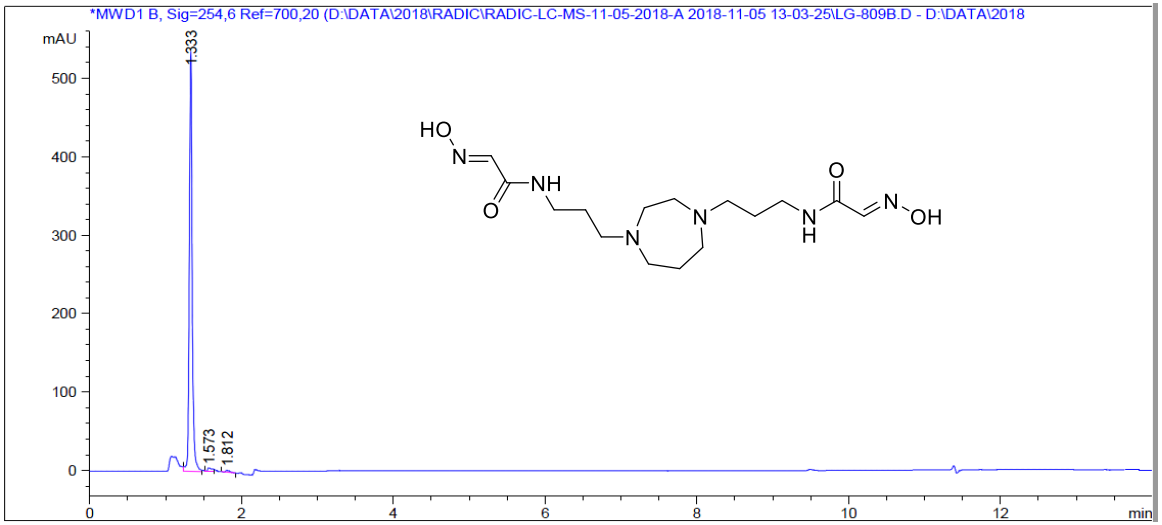

(2*E*)-2-(*N*-hydroxyimino)-*N*-[2-(1-{2-[(2*E*)-2-(*N*-hydroxyimino)acetamido]ethyl}piperidin-4-yl)ethyl]acetamide (LG-823) LC-MS purity:

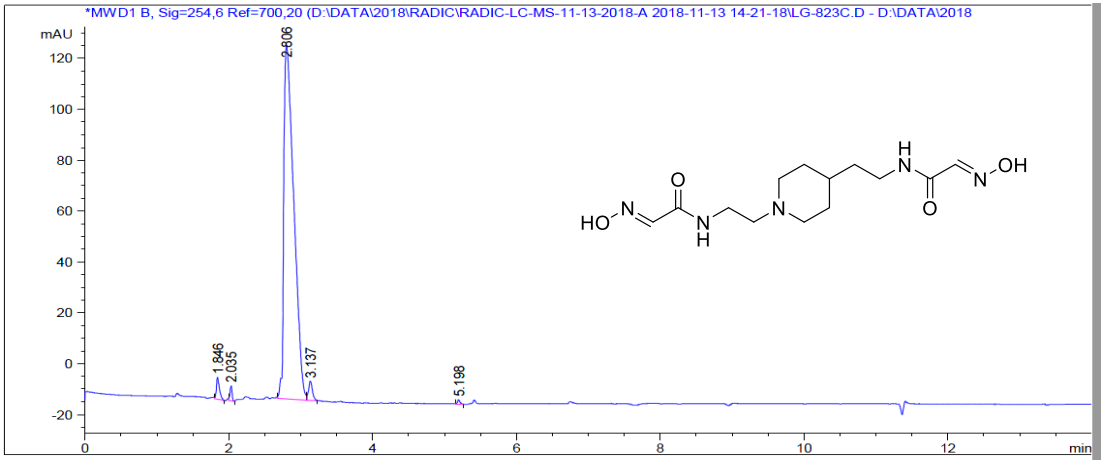

(2*E*)-2-(*N*-hydroxyimino)-*N*-[3-(4-{2-[(2*E*)-2-(*N*-hydroxyimino)acetamido]ethyl}piperidin-1-yl)propyl]acetamide (LG-829) LC-MS purity:

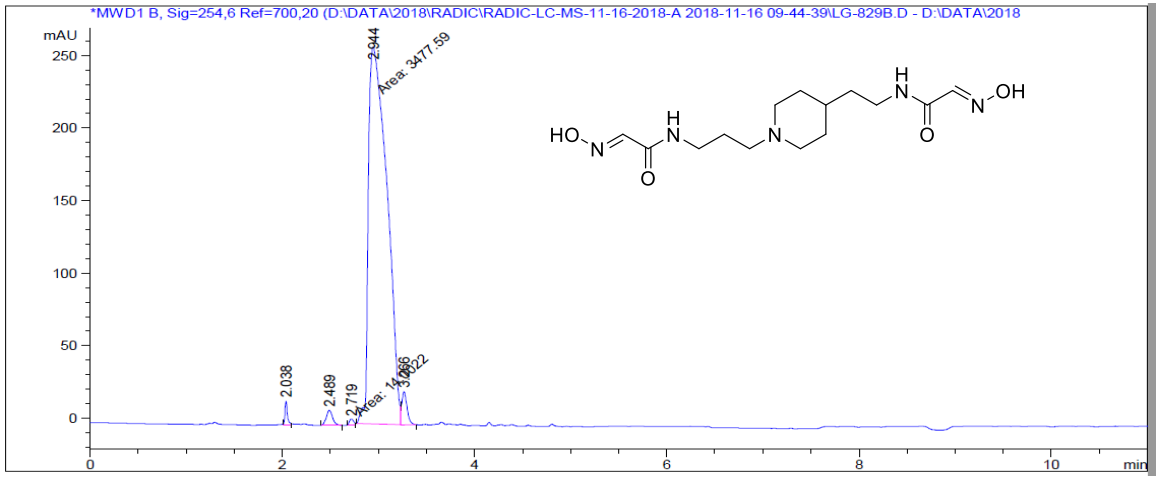

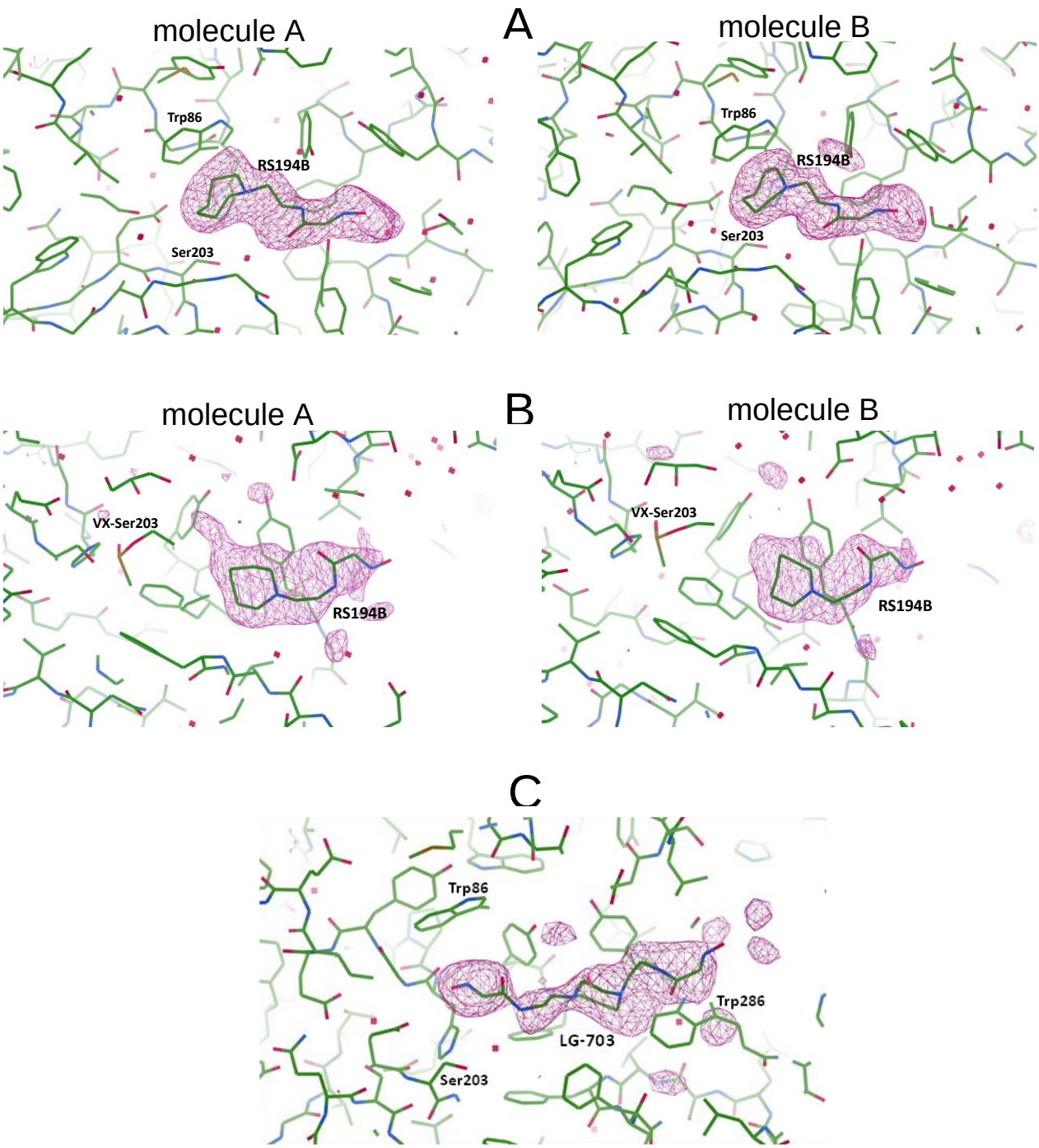

Figure S1. Polder omit F_O-F_C difference electron density maps of **A)** RS194B in hAChE*RS194B complex in molecules A (left) and B (right) (PDB ID 6U34) contoured at 4.5 σ level; **B)** RS194B in VX-hAChE*RS194B complex in molecules A (left) and B (right) (PDB ID 6U37) contoured at 4.5 σ level, and **C)** LG-703 in hAChE*LG-703 complex (PDB ID 6U3P) contoured at 3.5 σ level.

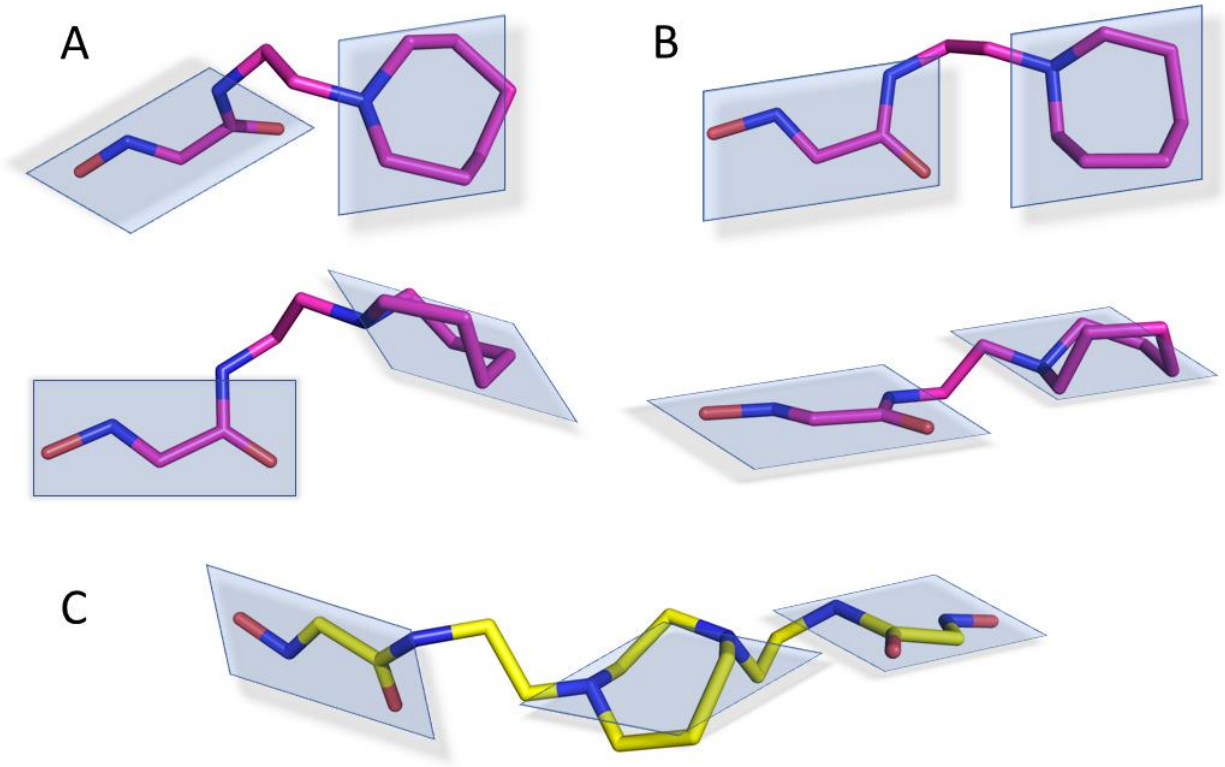

Figure S2. Different conformations of oxime reactivators in the studied complexes represented by average planes going through the oxime acetamido and saturated heterocycle groups. (A and B) Top and side views of RS194B complexed with apo and VX-inhibited hAChE, respectively. (C) Side view of LG-703 in the hAChE:LG-703 structure.

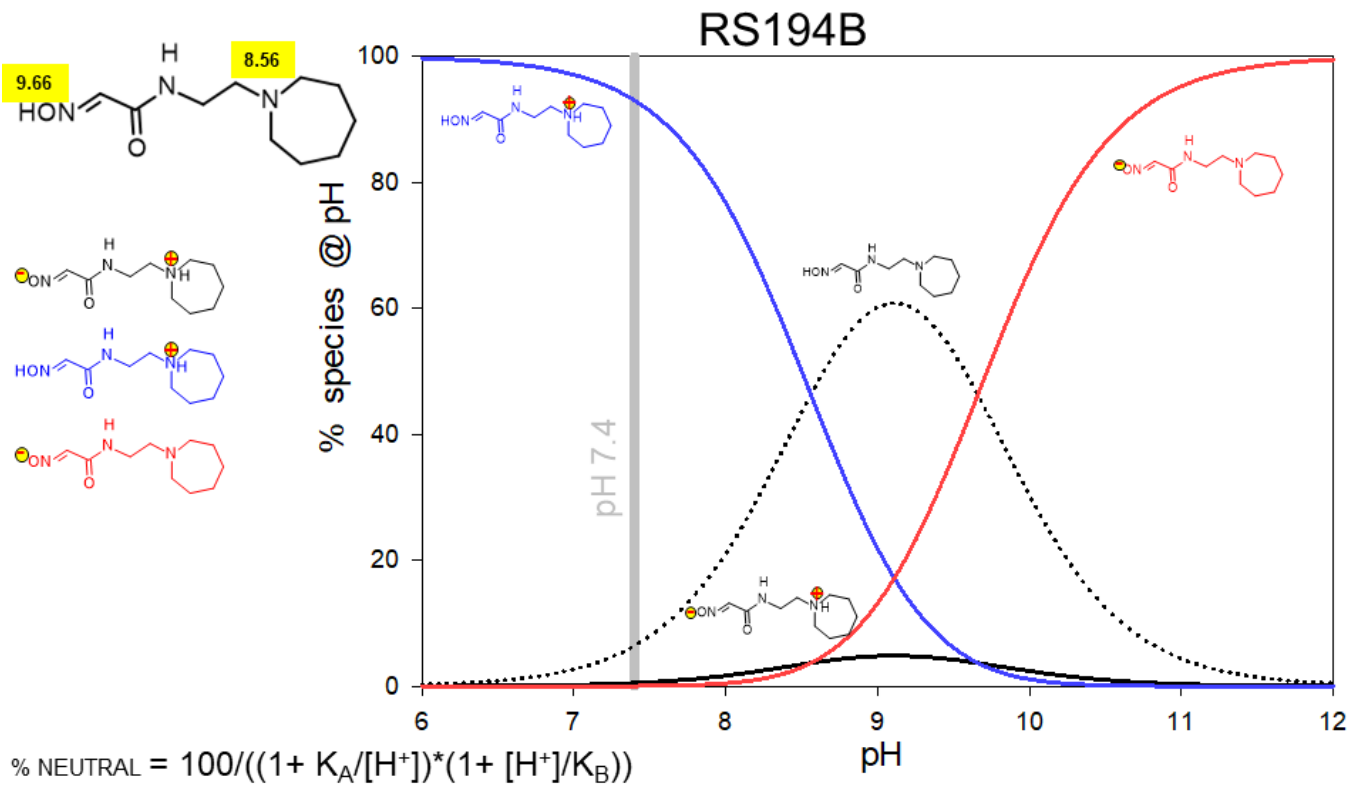

% NEUTRAL = $100/((1+ K_A/[H^+])*(1+ [H^+]/K_B))$

% ZWITTER = $100/((1+ [H^+]/K_A)*(1+ K_B/[H^+]))$

% CATION = $100/((1+ K_A/[H^+])*(1+ K_B/[H^+]))$

% ANION = $100/((1+[H^+]/K_B)*(1+ [H^+]/K_A))$

Figure S3. All four ionization forms of the monoxime RS194B generated by ionization of two groups, cyclic amine and oxime group. Individual pKa values determined experimentally are highlighted in yellow. Equations derived to calculate dependence of abundance of individual forms are based on dissociation constants of anionic (K_A) and cationic (K_B) ionization species.

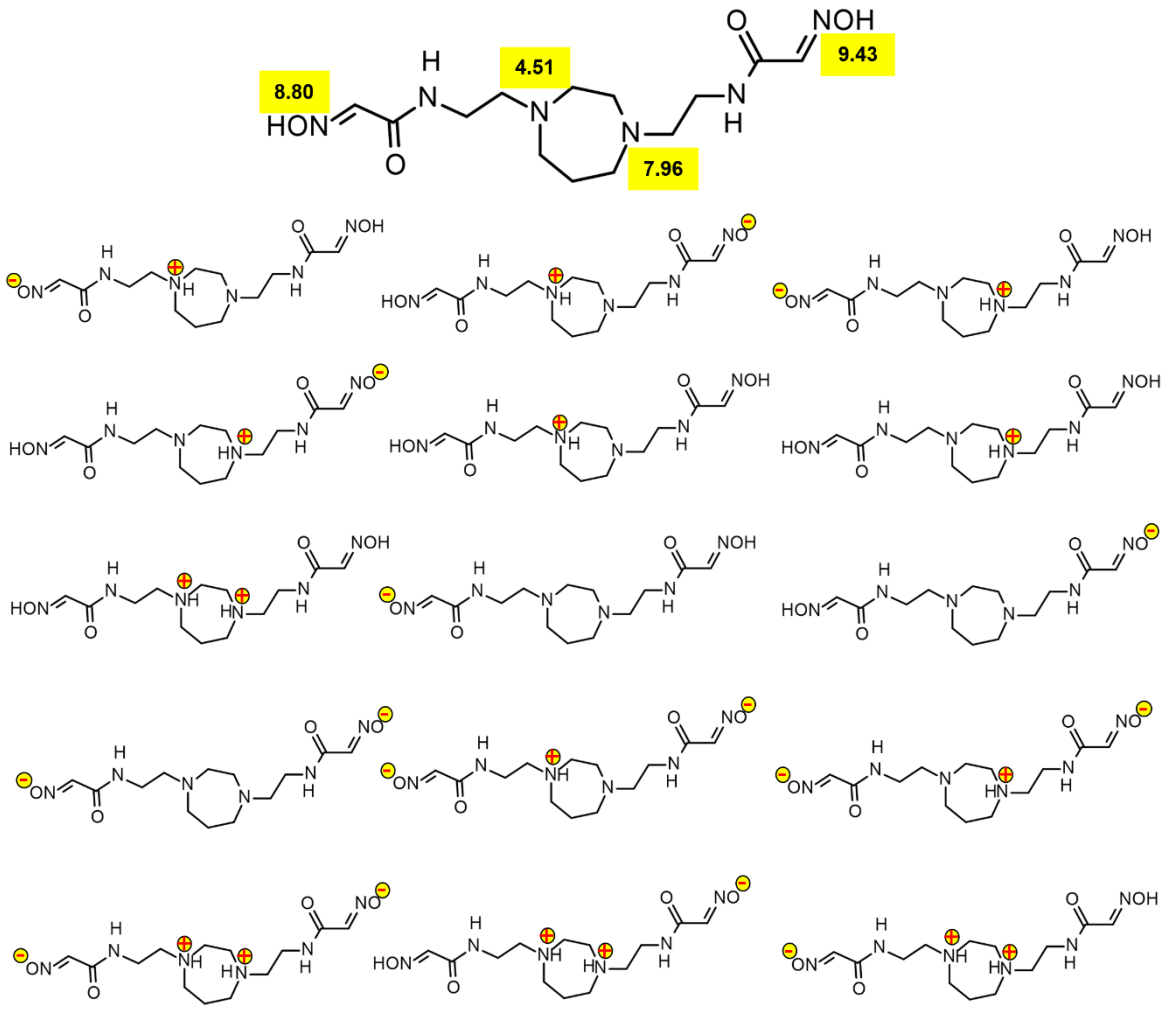

$$\%\ \text{NEUTRAL} = 100/[(1+ K_{A1}/[H^+])*(1+ [H^+]/K_{B1})*(1+ K_{A2}/[H^+])*(1+ [H^+]/K_{B2})]$$

$$\%\ \text{ZWITTER 1} = 100/[(1+ K_{A1}/[H^+])*(1+ [H^+]/K_{A2})*(1+ K_{B1}/[H^+])*(1+ [H^+]/K_{B2})]$$

$$\%\ \text{ZWITTER 2} = 100/[(1+ K_{A2}/[H^+])*(1+ [H^+]/K_{A1})*(1+ K_{B1}/[H^+])*(1+ [H^+]/K_{B2})]$$

$$\%\ \text{CATION}^{+1}1 = 100/[(1+ K_{A1}/[H^+])*(1+ [H^+]/K_{B1})*(1+ K_{A2}/[H^+])*(1+ K_{B2}/[H^+])]$$

$$\%\ \text{CATION}^{+1}2 = 100/[(1+ K_{A1}/[H^+])*(1+ K_{B1}/[H^+])*(1+ K_{A2}/[H^+])*(1+ [H^+]/K_{B2})]$$

$$\%\ \text{ANION}^{-2} = 100/[(1+ [H^+]/K_{A1})*(1+ [H^+]/K_{B1})*(1+ [H^+]/K_{A2})*(1+ [H^+]/K_{B2})]$$

$$\%\ \text{ANION}^{-1}1 = 100/[(1+ K_{A1}/[H^+])*(1+ [H^+]/K_{B1})*(1+ [H^+]/K_{A2})*(1+ [H^+]/K_{B2})]$$

$$\%\ \text{ANION}^{-2}2 = 100/[(1+ [H^+]/K_{A1})*(1+ [H^+]/K_{B1})*(1+ K_{A2}/[H^+])*(1+ [H^+]/K_{B2})]$$

Figure S4. All sixteen ionization forms of bis-oxime LG-703 generated by ionization of four groups, two cyclic amines and two oxime groups. Individual pKa values determined experimentally are highlighted in yellow. Equations derived to calculate dependence of abundance of individual forms are based on dissociation constants of anionic (K_{A1}, K_{A2}) and cationic (K_{B1}, K_{B2}) ionization species.

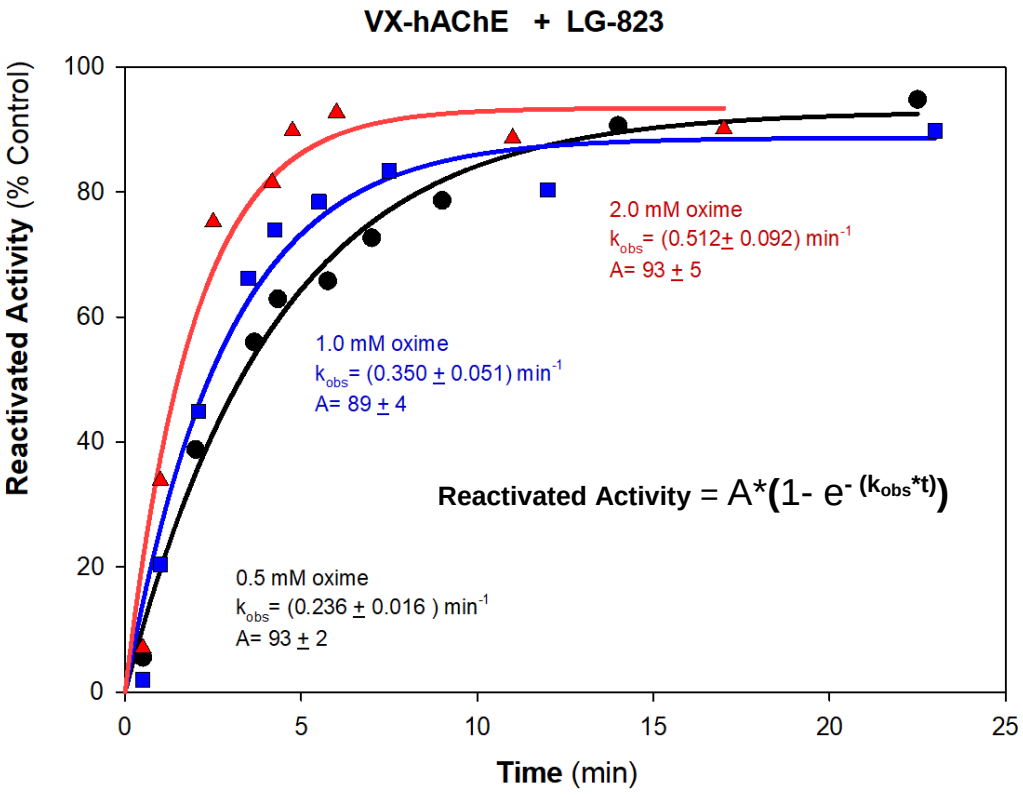

Figure S5. Time course of reactivation of VX-hAChE conjugate by three concentrations of the bis-oxime LG-823, 0.5 mM, 1.0 mM and 2.0 mM. Representative plot showing one experiment. Each curve was calculated by non-linear regression using the equation above and resulting k_{obs} constants plotted vs. oxime concentration, as shown in the Figure 6, in order to evaluate reactivation constants k_2, K_{ox} and k_r summarized in the Table 3.

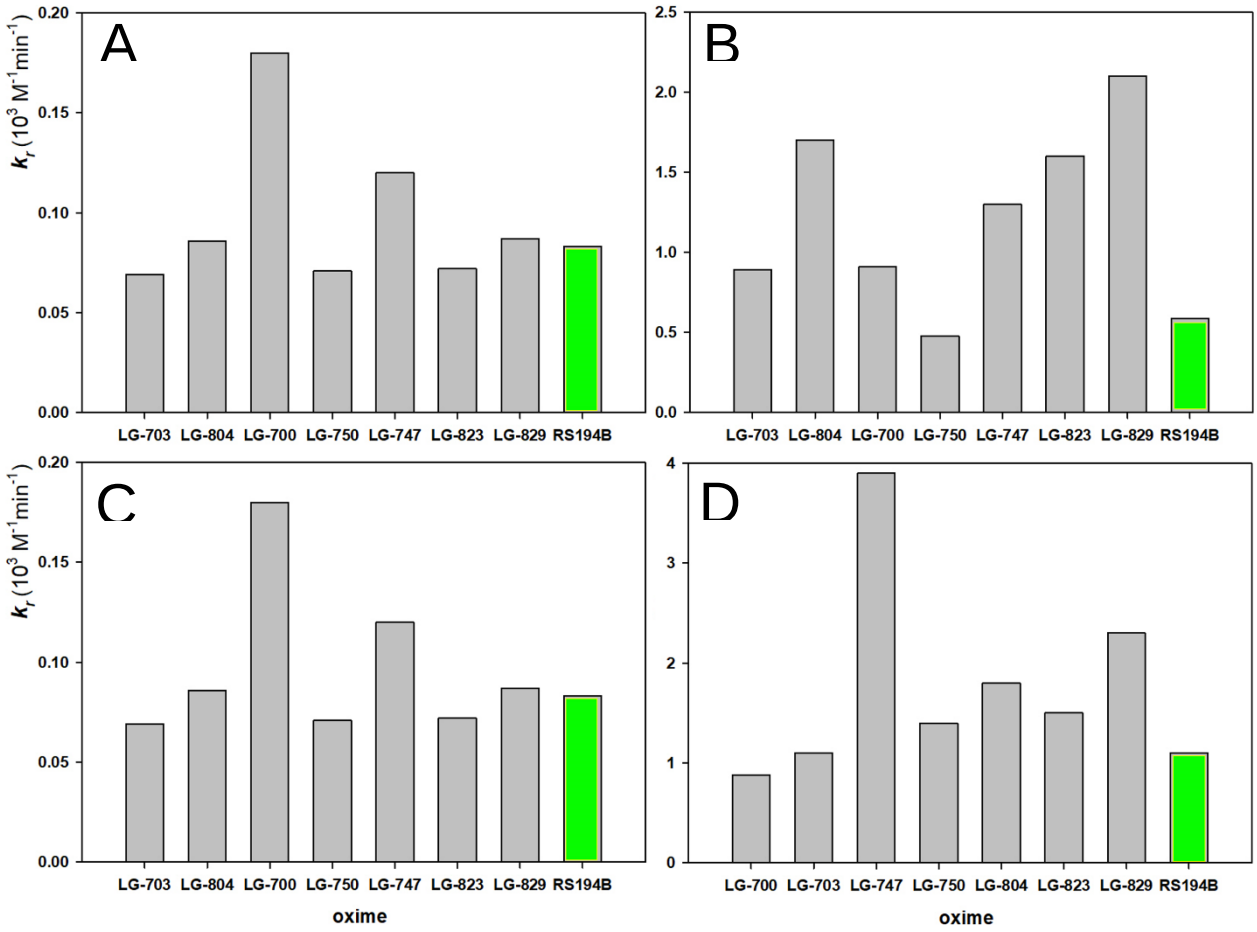

Figure S6. The second order rate constants (k_r) of LG bis-oximes (grey bars) compared to monoxime RS194B (green bars) for reactivation of A) Paraoxon-hAChE conjugate, B) Sarin-hAChE conjugate, cyclosarin-hAChE conjugate and VX-hAChE conjugate. Taller bars indicate better reactivation.

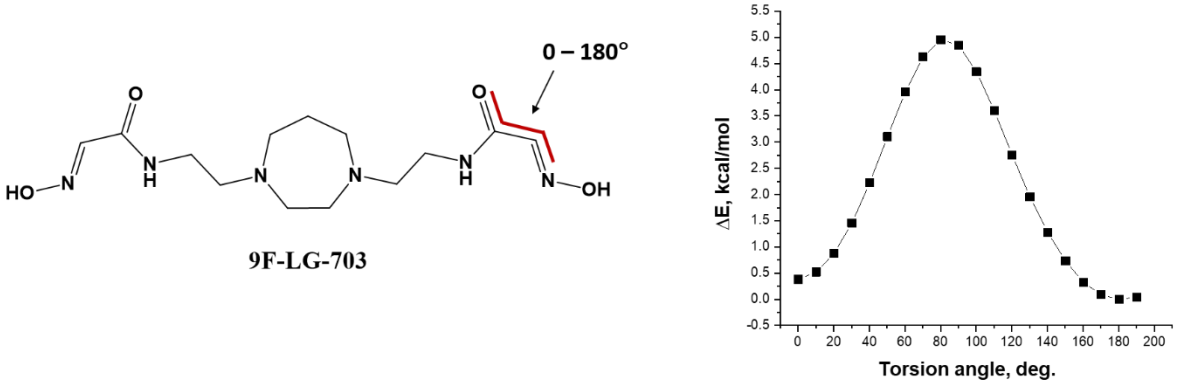

Figure S7. Torsion scan with QM in implicit water indicating that the LG-703 conformer with the trans conformation of the dihedral angle highlighted in red corresponds to the global energy minimum, whereas the cis conformer is 0.3 kcal/mol less stable. The energy barrier of the dihedral rotation is 5 kcal/mol.

Table S1. *In silico* design and evaluation of uncharged *bis*-oximes by computational docking into the VX-hAChE X-ray structure. Each compound was docked in four different *bis*-oxime protonation states. Compounds are rank-ordered using the average docking score.

Rank		Comp. #	Docking score				
			HON-NOH	-ON-NO-	HON-NO-	-ON-NOH	average
1	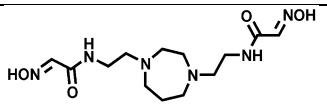	S5	0.3	-2.4	-2.3	-2.3	-1.7
2	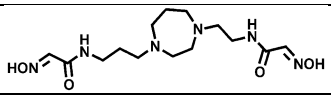	S7	-1.1	-1.4	-1.9	3.7	-0.2
3	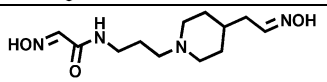	S11	-0.2	1.7	0.4	0.2	0.5
4	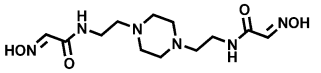	S16	-1.9	-2.2	3.6	3.2	0.7
5	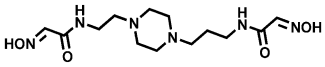	S17	0.1	-1.0	-1.9	5.7	0.7
6	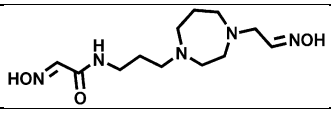	S3	1.7	-0.2	4.0	0.2	1.4
7	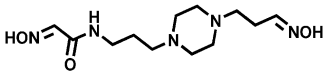	S14	0.5	0.1	5.8	0.3	1.7
8	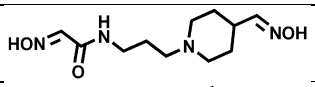	S10	-0.0	6.2	1.3	0.3	1.9
9	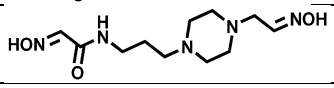	S12	0.9	0.3	1.6	5.1	2.0
10	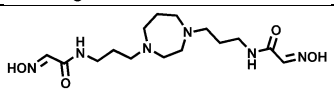	S6	0.1	-1.4	4.6	4.6	2.0
11	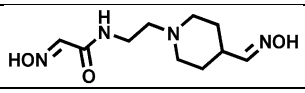	S8	2.6	0.5	1.1	3.8	2.0
12	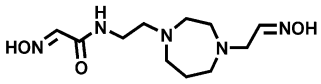	S1	5.4	3.8	0.9	-1.0	2.3
13	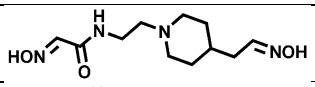	S9	0.4	7.9	1.0	0.8	2.5
14	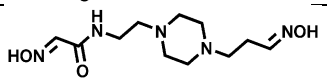	S15	-0.3	4.8	0.2	6.4	2.8
15	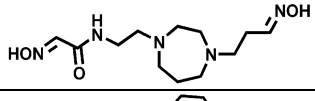	S2	-0.5	-0.1	6.7	7.8	3.5
16	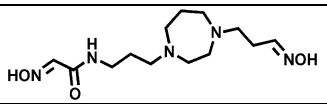	S4	2.9	0.0	6.6	7.1	4.2
17	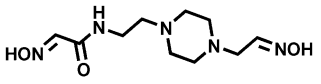	S13	0.2	8.0	0.5	8.8	4.4

Table S2. pK_a values of oxime groups obtained by oximolysis i.e. by nucleophilic degradation of 0.3 mM ATCh by 0.3 mM bis-oxime in phosphate-pyrophosphate buffers at pH 5, 6, 7, 7.5, 8, 8.5, 9, 9.5, 10, 10.5 and 11. Oximolysis rates obtained from 3 - 5 experiments at 22 ^{0}C were used for non-linear, bi-phasic (or monophasic for RS194B monoxime) regression analysis of "rate vs. pH" relationship (3) and resulting pK_a values and "Maximal nucleophilic reactivity" values with corresponding errors of the fit are given. For comparison, pK_a values from the Table 2 are also given, in italics and in smaller font.

oxime	pKa				Maximal nucleophilic reactivity
	Acid 1	Acid 2	Base 1	Base 2	(ΔA/min) per oximate
LG-703	*8.80* 8.91 ± 0.05	*9.43* 10.3 ± 0.1	*4.51*	*7.96*	0.278 ± 0.013
LG-804	*8.99* 8.98 ± 0.09	*9.59* 10.1 ± 0.2	*5.25*	*8.35*	0.213 ± 0.011
LG-700	*8.72* 8.97 ± 0.09	*9.23* 9.98 ± 0.18	*2.87*	*7.16*	0.208 ± 0.009
LG-823	*8.90* 9.05 ± 0.07	*9.45* 10.3 ± 0.2	-	*8.17*	0.214 ± 0.014
LG-750	*8.72* 8.95 ± 0.09	*9.39* 10.0 ± 0.2	*3.17*	*7.42*	0.234 ± 0.010
LG-829	*9.08* 8.82 ± 0.05	*9.86* 10.2 ± 0.1	-	*8.57*	0.204 ± 0.007
LG-747	*8.77* 9.78 ± 0.05	*9.42* 10.5 ± 0.1	*3.69*	*7.67*	0.208 ± 0.009
RS194B	-	*9.66* 9.28 ± 0.08	-	*8.56*	0.213 ± 0.009

Table S3. Stepwise structure-based design of uncharged bis-oxime antidotes against OP intoxication.

Step	Action	Outcome	Next step
1	X-ray structure of the RS194B*hAChE complex solved to create structural template for improvement of RS194B reactivation.	RS194B found in a "non-productive" orientation, with reactive oxime group pointing away from the site of OP conjugation (Ser203).	Verify RS194B orientation in the complex with OP conjugated hAChE (VX-hAChE).
2	X-ray structure of the RS194B*VX-hAChE complex solved to serve as a better template for improvement of RS194B reactivation.	Again, RS194B found in a "non-productive" orientation, with reactive oxime group pointing away from the site of VX conjugation (Ser203-VX). Just like in the structure in the step 1.	Introduce additional acetamidoxime (or similar) substituent into the central heterocyclic ring of RS194B in order to "force" at least one oxime group into the AChE active center gorge, to point towards the OP conjugation site (Ser203).
3	17 novel bis-oxime structures created *in silico* by adding the second oxime-group-containing "arm" to the central saturated heterocycle. Each oxime was docked computationally into the VX-hAChE structural template from the step 2.	The 17 bis-oximes computationally rank ordered, based on reactivation reaction dependent docking score (Table S1). The compound "S5", a symmetric acetamido bis-oxime based on RS194B structure, scored the best *in silico*.	Prepare bis-oxime material for *in vitro* reactivation efficacy test of the best *in silico* ranking bis-oximes.
4	The synthetic procedures were developed for the compound "S5", for three other bis-oximes from the Table S1, and for three additional heterocyclic acetamido bis-oximes.	Total of seven novel acetamido bis-oxime compounds were prepared in 20 – 150 mg quantity.	Use prepared bis-oxime material for *in vitro* reactivation testing of OP conjugated hAChE.
5	The *in vitro* reactivation potency for each of seven bis-oximes was tested against four OP-hAChE conjugates (VX-hAChE, sarin-hAChE, cyclosarin-hAChE, POX-hAChE) and compared to RS194B.	More than half of seven bis-oximes were more efficient reactivators than RS194B, in particular LG-829, LG-823 and LG-703 (Table 3).	Evaluate physico-chemical properties of bis-oximes in order to reveal their potential to diffuse across biological membranes and to nucleophilically reactivate OP-hAChE in tissue.
6	Several physico-chemical properties of bis-oximes evaluated experimentaly by potentiometric titration , including pKa and pKb determination of oxime groups and heterocyclic amines, compound *log*$D_{7.4}$ and *log*$P_{neutral}$ values as well as the composite CNS MPO index (Table 2).	Based on pKa and pKb values each of seven bis-oximes is expected to have significantly higher fraction of both uncharged and zwitterionic forms at pH 7.4 compared to RS194B, allowing for better diffusion across biological membranes and better nucleophilic reactivity. CNS MPO indexes were comparable to the one determined for RS194B.	Verify whether orientation of one of novel bis-oximes in the complex with hAChE turned from "non-productive" to "productive".
7	X-ray structure of the LG-703*hAChE complex solved to determine position of two oxime groups.	LG-703 found in a "productive" orientation, with one of the reactive oxime groups steered deep into hAChE active center, next to the Ser203 (Figure 7).	

14. Comparison of non-crystallographic monomers A and B of hAChE*LG-703

Interestingly, we found that LG-703 binds only to one of the two molecules in the asymmetric unit, monomer A, in the structure of LG-703 with apo-hAChE. This gave us a unique opportunity to compare the complex and the apo hAChE structures, both derived from the same crystal. The superposition of the two monomers is shown in Figure S5. The LG-703 binding resulted in the cascade of conformational changes in the side chains of residues lining the surface of the active site gorge above and including the "choke point". The most flexible side chains are those of Tyr337and Tyr124, the pair which defines the gorge choke point, Leu76 and Tyr77, the residues from the omega loop, and Tyr341. An interesting observation is that the reactivator binding resulted in the widening of the bottleneck that separates the catalytic and peripheral sites. The O…O distances between the phenolic side chains of Tyr124 and Tyr337 are 5.4 Å and 6.3 Å in the apo-like monomer B and complexed with LG-703 monomer A, respectively. This is in line with our previous observations on hAChE (4) and observations of others on mouse AChE and *Torpedo californica* AChE that binding of

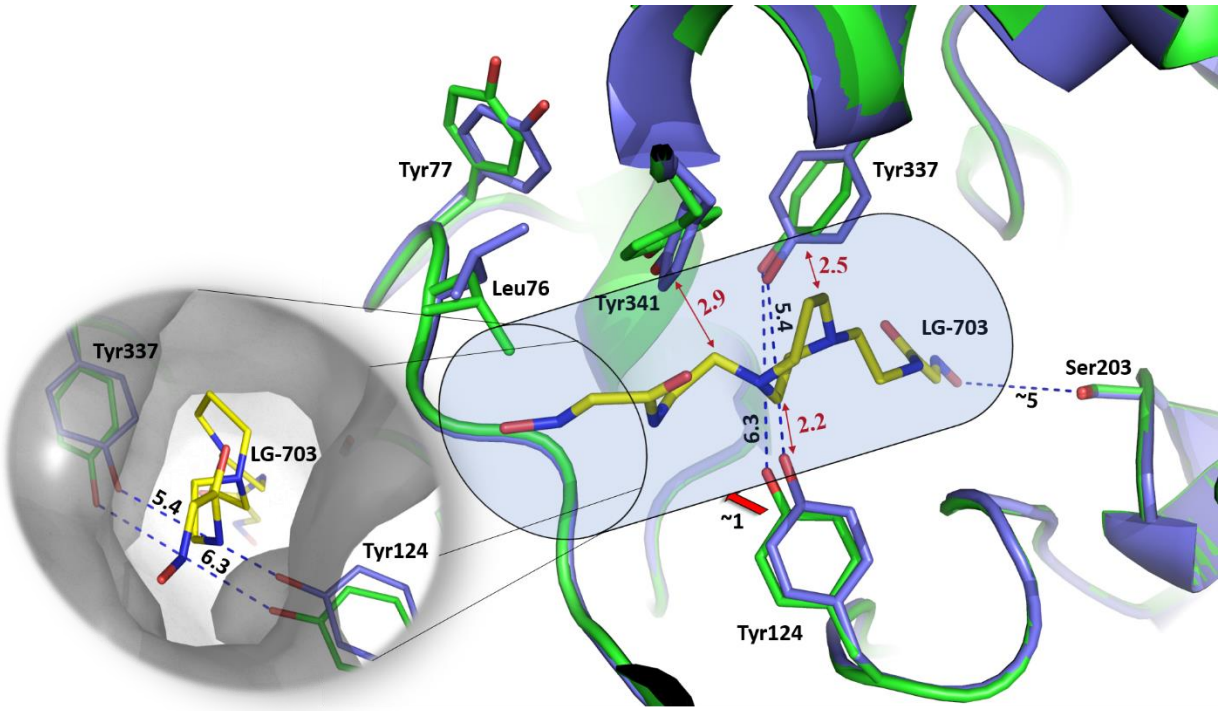

Figure S8. Binding of LG-703 forces expansion of the active site gorge bottleneck at the "choke point", defined by the distance between Tyr124 and Tyr337 side chains. Overlay of the monomers A (green carbons) with bound LG-703 (yellow carbons) and B with no ligand present from the binary hAChE*LG-703 complex. Insert shows the top view of the entrance to the active site gorge.

elongated ligands that span the base of the gorge and its opening (like donepezil, BW286c51 or similar) stabilize rotamers of the choke point aromatic residues (primarily Tyr337) in a largely open position. The second order association rate constants of those ligands with AChEs, as well as those ligands that bind to the lower part of the gorge only and have to traverse the choke point, are in the range limited largely by their diffusion through the bulk solvent (5) suggesting that conformational changes leading to choke point opening and closing are fast, do not require significant energy and are not limiting in interaction kinetics of those ligands with AChEs.

15. References

1. Sit, R. K.; Radić, Z.; Gerardi, V.; Zhang, L.; Garcia, E.; Katalinić, M.; Amitai, G.; Kovarik, Z.; Fokin, V. V.; Sharpless, K. B.; et al. New Structural Scaffolds for Centrally Acting Oxime Reactivators of Phosphylated Cholinesterases. *J. Biol. Chem.* **2011**, *286* (22), 19422–19430. https://doi.org/10.1074/jbc.M111.230656.

2. Filosa, R.; Peduto, A.; Micco, S. D.; Caprariis, P. de; Festa, M.; Petrella, A.; Capranico, G.; Bifulco, G. Molecular Modelling Studies, Synthesis and Biological Activity of a Series of Novel Bisnaphthalimides and Their Development as New DNA Topoisomerase II Inhibitors. *Bioorg. Med. Chem.* **2009**, *17* (1), 13–24. https://doi.org/10.1016/j.bmc.2008.11.024.

3. Radić Z, Sit RK, Kovarik Z, Berend S, Garcia E, Zhang L, Amitai G, Green C, Radić B, Fokin VV, Sharpless KB, Taylor P. Refinement of structural leads for centrally acting oxime reactivators of phosphylated cholinesterases. J Biol Chem. 2012, 287:11798-809.

4. Gerlits O, Ho KY, Cheng X, Blumenthal D, Taylor P, Kovalevsky A, Radić Z. A new crystal form of human acetylcholinesterase for exploratory room-temperature crystallography studies. Chem Biol Interact. 2019, 309:108698.

5. Radić, Z., Taylor, P. Interaction kinetics of reversible inhibitors and substrates with acetylcholinesterase and its fasciculin 2 complex. J Biol Chem. **2001**, 276: 4622-33.